Sustainable Materials and Technologies 41 (2024) e01003

Contents lists available at ScienceDirect

Sustainable Materials and Technologies

journal homepage: www.elsevier.com/locate/susmat

Cd-free kesterite solar cells: State-of-the-art and perspectives

G. Tseberlidis *, C. Gobbo, V. Trifiletti, V. Di Palma, S. Binetti

Department of Materials Science and Solar Energy Research Center (MIB-SOLAR), University of Milano-Bicocca, Via Roberto Cozzi 55, 20125 Milano, Italy

ARTICLE INFO

Keywords:
Kesterite
Cd-free
Solar cell
Buffer layer
Perspectives

ABSTRACT

In the scenario of the new emerging photovoltaics, kesterites play a lead role in the thin-film solar cell technologies. This class of compounds, mainly represented by the pure-sulfide form Cu_2ZnSnS_4 (CZTS) and the sulfo-selenide form $Cu_2ZnSn(S,Se)_4$ (CZTSSe), shows unique characteristics and stands as a promising p-type absorber material thanks to its high absorption coefficient, high cost-effectiveness and low toxicity. However, CdS is commonly used as the n-type partner (buffer layer) in kesterite solar cells but, beyond its toxicity, it has a nonoptimal band alignment with kesterites and exhibits parasitic absorption at low wavelengths due to its bandgap. Several efforts have been made in the last decade, to replace CdS with a suitable, Cd-free, both environmentally and economically sustainable buffer layer, and many times with successful results allowing not only to equal, but also to overcome in few cases the performances of the corresponding CdS-based reference devices. $Zn_{1-x}Sn_xO$ for instance leads to higher efficiencies than CdS when coupled with pure-sulfide CZTS, while Zn(O,S) seems to couple better with CZTSSe. TiO_2 has been also considered as suitable buffer layer for kesterites and, in the last few years, several works have been reported both theoretical and experimental, showing very promising results. In this review we summarize the efforts and the improvements recorded by the scientific community working on this topic in the last ten years, with the aim to supply a landmark useful to design future experiments in a more efficient way and to push forward the related research activities, in order to fully overcome CdS limitations and to promote thin-film kesterite devices to higher performances.

1. Introduction

Kesterite absorbers, mainly represented by Cu_2ZnSnS_4 (CZTS), $Cu_2ZnSn(S,Se)_4$ (CZTSSe) and $Cu_2ZnSnSe_4$ (CZTSe), are a class of fully inorganic materials interesting for the large-scale production of thin film photovoltaic (PV) technology, thanks to their high absorption coefficient (over 10^4 cm^{-1}), their direct band gap energy, which can be tuned between 1.0 and 1.6 eV, by modifying the [S]/([S] + [Se]) composition, their natural p-type conductivity, their minimum material usage and earth-abundance [1]. To date, the record efficiency for the selenized kesterite with low bandgap is 14.9%, while the best efficiency for pure sulfide CZTS, with higher bandgap, is 11.4% [2]. Several research groups have devoted significant efforts towards the increasing of the kesterite-based solar cells PV performances, which is necessary for industrial implementation [3–10]. Kesterite materials, due to their structural similarity, are strictly related to the already available at commercial stage $CuInGaSe_2$ (CIGS), while based on abundant, environmentally friendly and low-cost elements [11]. In the future scenario of the "Terawatt Era", PV will play a lead role in many applications, including Product Integrated Photovoltaics (PIPV), such as "wearables", building integrated photovoltaics (BIPV) and vehicle integrated photovoltaics (VIPV), where light-weight thin-film technologies are mandatory. Considering the production costs of CIGS deriving from the scarcity of some of its composing elements (In and Ga), or the toxicity related to CdTe, it would not be reliable to base the whole inorganic thin-film PV technology on these absorbers. This issue prompted the scientific community to investigate kesterites as a valid low-cost alternative and, little-by-little, the efficiencies have been improved reaching the current record of $\eta = 14.9\%$[2,12,13]. Given their apparent structural similarity, the device architecture used for kesterites was first derived from the one developed for CIGS, even if is not so ideal for them. In particular, many works are aimed at designing a buffer layer that can enhance charge extraction and, thus, all PV parameters. Currently, CdS is the standard buffer layer used in CZTS and CZTSSe solar cells, nevertheless Cd is toxic and produces hazardous waste and byproducts from the solution-based chemical bath deposition (CBD) process, damaging the environment and health [14]. In addition, it has a narrow bandgap (2.4-2.5 eV), which reduces the amount of light reaching the absorber and introduces

* Corresponding author.
E-mail address: giorgio.tseberlidis@unimib.it (G. Tseberlidis).

https://doi.org/10.1016/j.susmat.2024.e01003
Received 14 December 2023; Received in revised form 11 April 2024; Accepted 31 May 2024
Available online 3 June 2024

parasitic absorption in the UV range [15]. Moreover, especially for S-rich absorbers, the lattice mismatch between CdS and kesterite interface is quite high (~ 7% for CZTS and ~ 2.4% for CZTSe), thus producing interfacial defects and limiting devices performances [16,17]. CdS has a nonoptimal cliff-like band alignment with CZTS, thus resulting in an open circuit voltage (V_{OC}) deficit [18–23]. The higher PV parameters are recorded for the selenized kesterite compared to the sulfide ones, thanks to a more suitable CdS/CZTSSe band-alignment [24]. To minimize photon losses and to achieve higher efficiencies, CdS should be replaced with a n-type material with wider band gap and/or higher Valence Band Maximum (VBM) and Conduction Band Minimum (CBM) values [21,24]. In the last decade, several efforts have been made, in order to find a suitable Cd-free substitute of CdS, eco-compatible, economic, earth-abundant buffer layer [24–28]. In this scenario, alternative buffer layers such as $Zn_{1-x}Sn_xO$ (ZTO)[29], Zn(O,S)[30], ZnS [31], Ins_2S_3 [26], and TiO_2 [32,33], have been investigated and studied to improve charge transport, make devices more sustainable and boost efficiencies even more. In many cases impressive results have been achieved, which allowed to equal or even overcome, the efficiencies of the corresponding CdS-containing reference devices. $Zn_{1-x}Sn_xO$ has been recorded as the best alternative buffer layer, so far, when paired with pure-sulfide CZTS [15,34,35], while Zn(O,S) leads to better efficiencies with CZTSSe [36–38]. In_2S_3 was also successfully studied, but despite the low thicknesses used, its indium content hinders its potential large-scale application [26,39–41]. On the other hand, economically sustainable ZnMgO has not been studied enough to allow performances as high as CdS so far [25,42,43]. Lastly, TiO_2 has been also considered as suitable buffer layer for kesterites and, in the last few years, several works have been reported both theoretical and experimental, showing very promising results [32,33].

In this review, we want to highlight not only the overall record efficiencies reached by using the above-mentioned alternative buffer layers, but to compare specifically its performance with the CdS-based reference device with all the other layers produced in the same way, by the same procedure, and the same research group. In this way, the direct comparison can help the reader to understand the true issue (i.e. CdS vs alternative buffer layers) instead of focusing just on the sterile number of a record efficiency. For example: a reference device with CZTS/CdS junction relying on $\eta = 5\%$ has to be compared with its corresponding CZTS/ZnSnO junction with $\eta = 5\%$, concluding that the two buffer layers equally perform, and that, even though 5% could be considered a low efficiency, it can be ascribed to other limitations of the devices (CZTS inner defects due to its deposition, problems at the interfaces other than the p-n junction, etc). This decision has been made, to highlight the excellent work of many research groups regarding the alternative buffer layers and to allow the readers to a better understanding of what will be the best alternative buffer layer for CZTS in order to push forward the research on this crucial topic and promote kesterites as the real alternative thin film solar cell for the terawatt generation of PV.

2. Kesterite thin film solar cell principles

A kesterite-based solar cell is generally produced by depositing a series of layers of different materials. Typically, the device architecture includes soda-lime glass (SLG) as the substrate, molybdenum as the back contact, kesterite as the light-absorbing layer, cadmium sulfide (CdS) as the buffer layer, intrinsic zinc oxide (i-ZnO) and aluminum-doped zinc oxide (ZnO:Al or AZO) as the window layer, plus an aluminum contact grid for the charge extraction (Fig. 1a). The back contact, whose function is to extract the holes generated by the absorber material, is usually the first layer to be deposited on the SLG substrate. Mo is the most commonly used material as a back contact since it is stable at high temperatures, ensures good adhesion of the light absorber layer and does not generate alloys with copper [1,29]. On the other hand, a MoS_2 or $MoSe_2$ layer between Mo and the kesterite is generated during the light-absorber annealing step, thus affecting the charge extraction [44]. Moreover, a Schottky contact can arise from the difference between the Mo work function and the one of CZTS, decreasing the built-in potential, increasing the dark current, and therefore reducing the V_{OC} (Fig. 1b) [45]. The short circuit current (J_{SC}) is instead affected by the band bending at the interface between Mo/CZTS, to which the photogenerated electrons are attracted and so recombining at the Mo surface. So, even though Mo is currently considered the best back contact for the reasons discussed, it can significantly reduce the performance of some kesterite-based devices [45]. The most commonly used strategy today is to modify the composition of the kesterite to tune the conduction bands of the light absorber with the back contact.

The kesterite is, indeed, directly deposited onto the molybdenum, with a thickness varying between 1.0 and 2.0 μm (Fig. 1a). This material can be obtained either by physical or chemical methods, as discussed later on. To complete the p-n junction, the buffer layer is then deposited, typically cadmium sulfide. Due to the toxic nature of cadmium, this layer, usually with a thickness of 50 nm, is deposited by chemical bath deposition as described in deep later on. Since the CdS layer is extremely thin and can have a rough surface, an intrinsic zinc oxide (i-ZnO) layer is deposited to prevent the back and top electrodes from coming into contact, thereby short-circuiting the device. Finally, a transparent conductive layer characterized by high transmittance and significant electrical conductivity, aluminum-doped zinc oxide (AZO), is used as a top contact to extract the electrons. Both i-ZnO and AZO are usually deposited by sputtering. Finally, to collect the photogenerated electrons, an aluminum grid is deposited by thermal evaporation (Fig. 1a).

The device core is the p–n junction composed of the kesterite and the

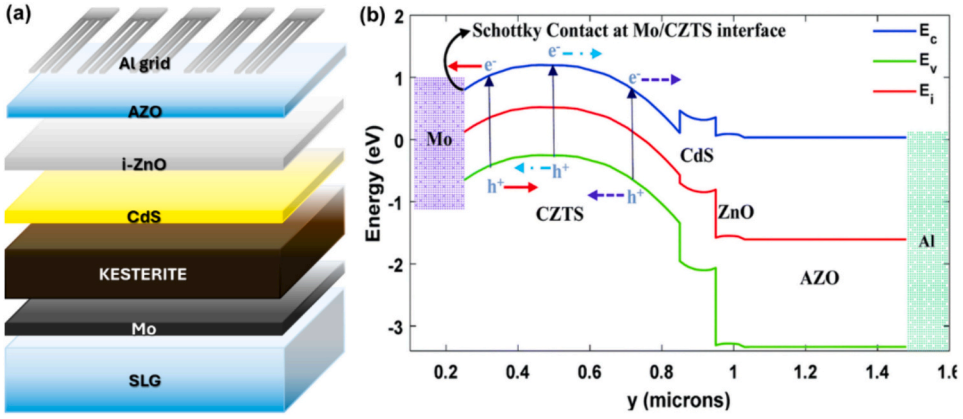

Fig. 1. (a) Typical structure of a kesterite-based solar cell; (b) band diagram of a CZTS-based solar cell: dotted arrows indicate the path that the charge should take to maximize the PV efficiency, and solid arrows refer to the path towards the wrong electrode (License CC BY 3.0)[45].

buffer layer, which can convert photons in electron-hole pairs. When a photon with energy higher than the band gap is absorbed, its energy excites an electron localized in the valence band to the conduction band, making it a free negative charge; in the meantime, the lack of the localized valence electron will create a hole. The electric field, due to the potential difference between the p-type and n-type material that make up the p-n junction, avoids the charge quenching, and decouples electrons and holes, directing them to the electrical contacts [46,47].

3. Kesterite thin film deposition

The first CZTS solar cell was reported by Katagiri and coworkers in 1997 with $\eta = 0.66\%$ [48], followed by a rapid increase to 12.6% efficiency in 2013 [12], until the current recent record of $\eta = 14.9\%$ in 2023 [2]. Despite vacuum-based methods were always considered as the best choice for the deposition of inorganic thin-film chalcogenides, this thought, inherited from the CIGS research era, slowly changed in favor of solution-based methods, when, starting from 2009, most record devices, including the current record, have been deposited by solution-based methods [12,13]. In fact, this is approach carries important advantages for looking to an industrial process for a mass-production given that solution-based methods are quite cheap and easily to scale-up. These depositions are based on a starting precursor solution/ink where metal chalcogenides, oxides or salts are dissolved in a suitable solvent. The solution is then deposited on a substrate (rigid or flexible) through different techniques, among them we find spin-coating, dip-coating and spray pyrolysis, dip-coating, ink-jet printing. This step is repeated a certain number of times, depending on the solution concentration and the technique used, in order to achieve the desired thickness and between one layer and the following one the solvent is usually removed by evaporation. To form the quaternary kesterite phase, the last step of the growth involves an annealing at high temperatures (450-600 °C) in inert atmosphere and in presence of S, Se or both, depending on the desired kind of kesterite. This last step is also shared with vacuum deposition approaches, where, after sputtering or evaporating the metal stacks, the kesterite phase is always formed through annealing at high temperatures in presence of S/Se. However, for the solution-based methods, the nature of the solution is crucial to achieve a high-quality absorber. Impurities, aggregates and/or wrong oxidation states of the metal precursors lead to poor quality kesterite thin films, while an incomplete removal of the solvent between to consecutive layer deposition can lead to cracks and/or inhomogeneities. The most common metal sources are salts (i.e. chlorides, acetates, acetylacetonates, nitrates) thanks to their high solubility in polar solvents. In Fig. 2 the most common kesterite thin-films deposition strategies have been grouped and reported.

It has to be highlighted that, in many cases, to obtain a pure-surface thin-film and high-efficiency devices, the samples undergo to chemical etching before the buffer layer deposition. The most efficient and common etching strategy involves KCN, which, however, due to its toxicity and dangerous nature is not applicable in every country due to strict regulations. Lastly, like other chalcogenides, doping and partial/total substitution of elements is frequently employed as a useful tool to enhance the PV performances of the final devices. Kesterites can be doped by introducing alkali metals such as Na, K and Li and it has been proved to be beneficial for grain growth, grain passivation and better adhesion to the substrates. On the other hand, cation substitution stands as a promising strategy to improve/modulate kesterite properties, such as the band gap. Naturally, thanks to their similar electronic configurations, elements of the same groups of the periodic table groups have been studied and reported more frequently, such as Cu-Ag, Zn-Fe, Zn-Mn or Ge-Sn [24].

4. CdS golden standard

Despite its toxicity, its parasitic absorption at low wavelengths and its non-optimal band alignment with kesterite, CdS still stands as the golden standard in kesterite thin-film solar cells, especially in substrate configuration. In fact, kesterites solar devices can be produced with two main architectures (Fig. 3): substrate configuration, where kesterite is grown on the back contact (conventionally Mo) with architecture "substrate/back contact/kesterite/buffer layer/top contact", or in superstrate configuration, where the absorber is grown on the buffer layer like "substrate/top contact/buffer layer/kesterite/back contact"[49]. Given the high annealing temperatures required to produce high crystallinity kesterites (> 550 °C) the substrate configuration is preferred over the superstrate, where in the latter the crystal phase of CdS can be easily degraded [50,51]. On the other hand, despite

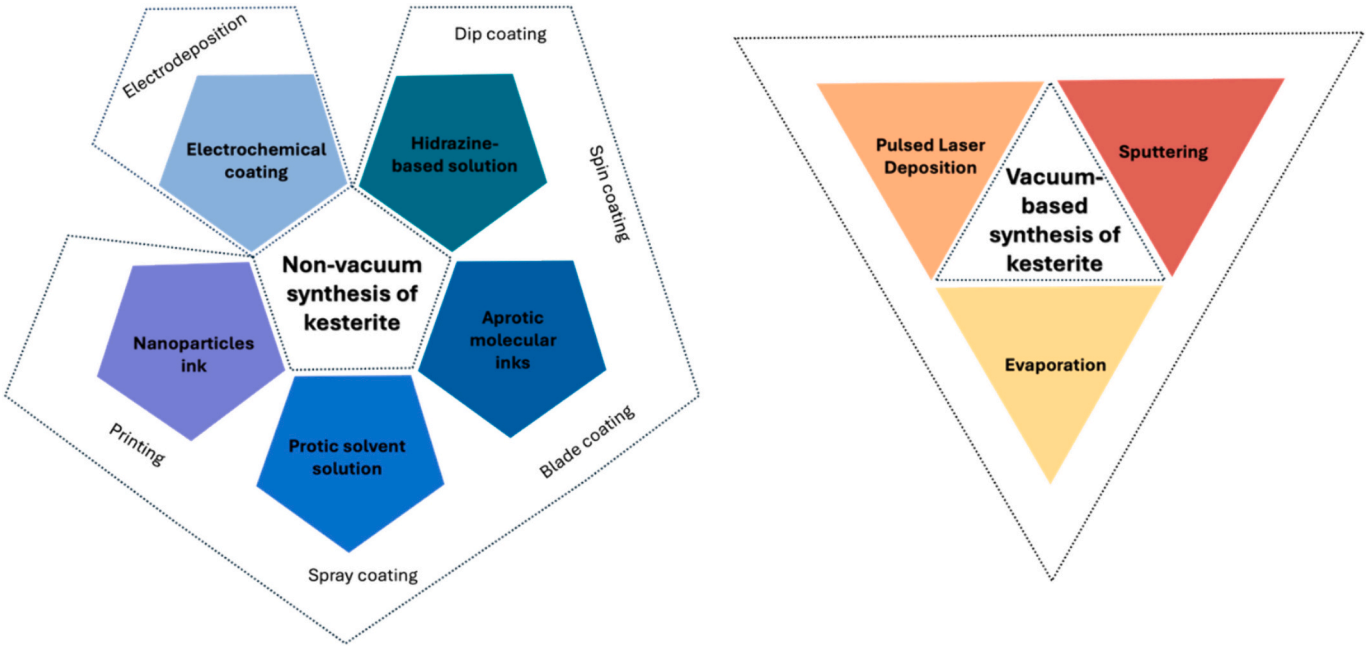

Fig. 2. The most common kesterite thin-film deposition strategies grouped in non-vacuum-based techniques VS vacuum-based ones.

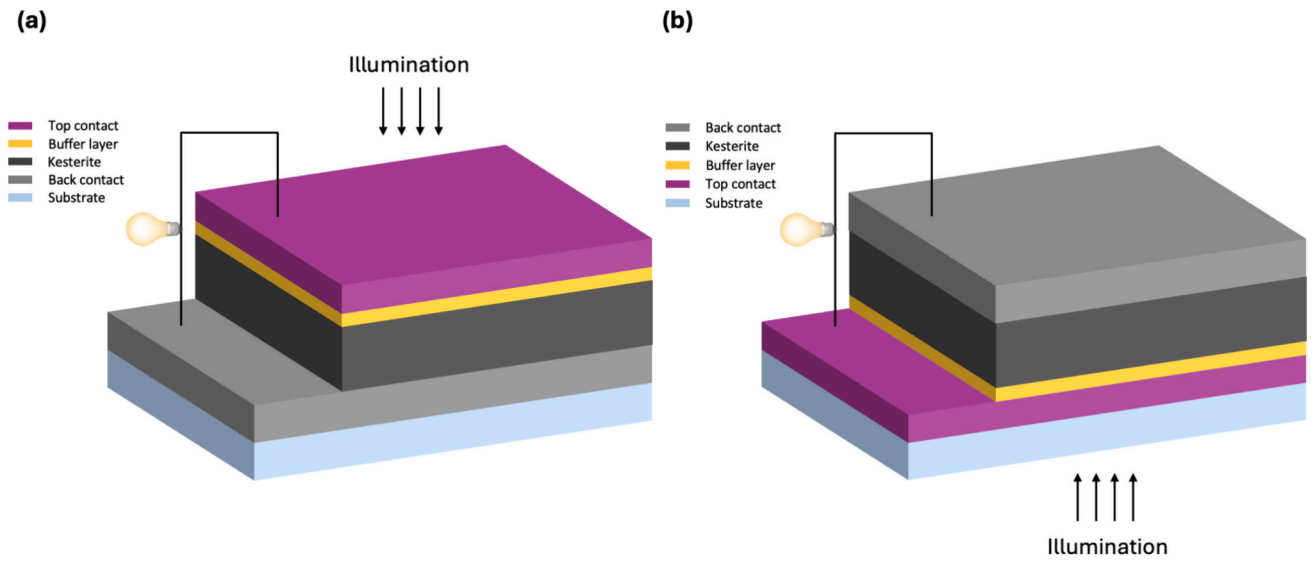

Fig. 3. (a) Substrate and (b) superstrate configuration architectures commonly used in the production of kesterite thin-film solar cells.

preserving CdS phase, substrate configuration discourages the use of Transparent Conductive Oxides (TCO) as back contacts (essential for bifacial and/or tandem applications) due to their possible heavy sulfurization and then degradation of them during the annealing [52,53]. However, to avoid so, interesting preventive strategies have been reported and in the last decade several works have been reported with devices built both in substrate and superstrate configuration, using back contacts other than Mo and sometimes with buffer layers alternative to CdS [33,49,52,53].

The most used growth method for CdS is Chemical Bath Deposition (CBD), where the substrates are dipped in a basic solution containing a cadmium salt, ammonia and thiourea at 70-80 °C for a limited amount of time until the desired thickness is reached [35,54,55]. With this buffer layer, record efficiencies have been reached for both CZTS and CZTSSe absorbers, of 11.4 and 14.9% respectively [2,12,13,56], with thicknesses ranging between 25 and 75 nm (Fig. 4). Annealing treatments on the so-formed p-n junction have been studied and reported, sometimes with successful results, enhancing the solar cell performance thanks to a diffusion layer at the interface. Cd diffusion into CZTS at the interface lead to the formation of of $Cu_2Cd_xZn_{1-x}SnS_4$ while Zn diffusion into CdS results in the formation of $Zn_xCd_{1-x}S$ evidently responsible for a better band-alignment between kesterite and CdS [13].

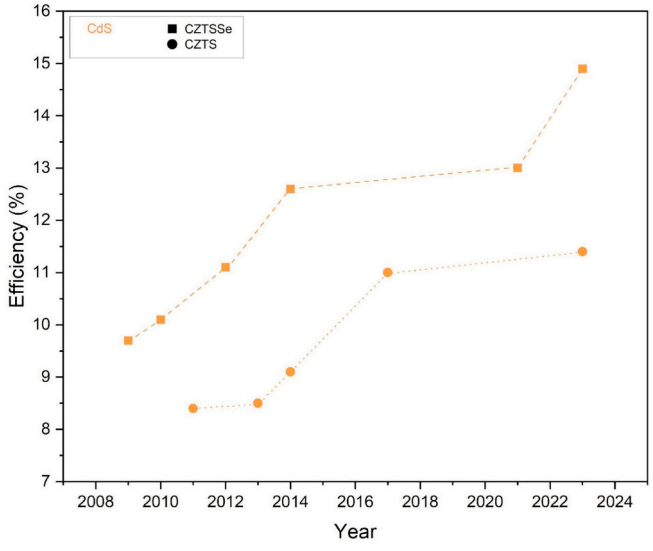

Fig. 4. Breakthrough in the kesterite thin film solar cells with commonly used CdS buffer layer.

5. CdS band alignment with kesterites

The buffer/kesterite interface band alignment engineering is a key factor in the production of high-efficiency solar cells. As depicted in Fig. 5a and b, the conduction band offset (CBO) between CdS and CZT(S,Se) can have a cliff-like configuration (kesterite CB edge is higher than that of the buffer layer) or a spike-like one (kesterite CB edge is lower than that of the CdS). It has been reported that the cliff-like conformation is detrimental for the electrons' injection, shrinking the V_{OC}, meanwhile, the spike-like has been proven to be beneficial in reducing the charge recombination at the interface [24,57,58]. More in detail, the CBO values for having highly efficient solar cells have been calculated to be between −0.1 eV and + 0.3 eV. CBO lower than −0.1 eV increases the charge carrier recombination. The CZT(S,Se) bandgap can be tuned by varying the [S]/([S] + [Se]) ratio, and as a consequence also the band alignment will change. Platzer-Björkman et al., described the band edges' evolution following the [S]/([S] + [Se]) ratio variation, collecting calculated and observed CBO and VBO, as shown in Fig. 5c [24]. For the pure sulfide form, CZTS, some reports show that CBO can be spike-

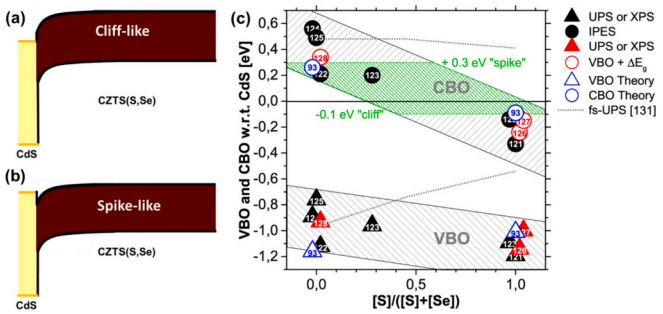

Fig. 5. Conduction band offset between CdS and CZT(S,Se) in (a) cliff-like and (b) spike-like configurations. (c) Direct measurements, estimated and calculated values of VBO and CBO between CdS and CZT(S,Se), varying the [S]/([S] + [Se]) ratio: the calculated CBO range for high-efficiency devices is depicted in green (Charlotte Platzer-Björkman et al.[24], available under the terms of the Creative Commons Attribution 3.0 license at doi:https://doi.org/10.1088/2515-7655/ab3708).

like, but most of the time it is a cliff-like alignment. On the contrary, for the pure selenide form, CZTSe, CBO is always a spike-like configuration. Calculations suggest that the CBO should range between −0.1 and + 0.3 eV to have high-performance devices: values lower than −0.1 eV will increase the charge carrier recombination and CBO larger than +0.3 eV will create a barrier for the electron transport. The CBO for the mixed composition, CZT(S,Se) varies as the composition is tuned from being cliff-like for high S content to spike-like as the Se amount increases.

In conclusion, one of the reasons why the CZT(S,Se)-based devices are the performance leader in the kesterite PV research, is the more beneficial band alignment with CdS compared with the pure S counterpart. Lately, the CZTS cation substitution strategy has been applied to move the CBO to a more favorable alignment with CdS [44,59–67]. For example, Cu partial substitution with Ag has been proven to be able to shift the CdS/CZTS CBO from −0.25 eV to −0.11 eV for CdS/(Ag,Cu)ZTS [68].

6. Cd-free alternative buffer layers

As already mentioned, despite the records reached by the kesterite/CdS junction, CdS is one of the main issues regarding the modest performances of kesterite solar cells due to its non-optimal band alignment (especially with CZTS), its narrow band gap (2.4 eV) and its parasitic absorption in the region between 400 and 500 nm [24,68–71]. Several attempts have been made to substitute it with other buffer layers, sometimes with exciting results. For instance, the employment of $Zn_{1-x}Sn_xO$ lead to high efficiencies comparable to those achieved with CdS, especially for high band-gap kesterites, CZTS [15,34,35]. Zn(O,S) family compounds have been also widely studied as buffer layers, but with more modest results compared to $Zn_{1-x}Sn_xO$, matching better with lower band-gap kesterites (CZTSSe) and very dependent on the deposition technique used [36–38]. Among the others, In_2S_3 showed interesting results indeed, but resulting in the replacement of a cheap buffer layer like CdS with an expensive In-containing one leading to even lower performances [26,39–41]. In the last few years, TiO_2 has been considered as a suitable buffer layer for thin-film kesterite solar cells thanks to several simulations where the theoretical efficiency of the devices could achieve values close to 15% (considering a common and naturally defective kesterite)[72]. From the experimental point of view, few works have been reported but recently very promising results have been achieved [32,33]. ZnMgO has been barely studied and reported, despite its potential to replicate the beneficial effects showed when coupled with CIGS [25,42,43,73]. A few other materials have been reported where Cd was still present mixed with other elements or stacked as thinner CdS window layer at the p-n junction between kesterite and the n-type chosen semiconductor to be coupled with, such as CdZnS and In_2S_3/CdS [74–76]. In these cases, good results were obtained thanks to the enlargement of the buffer layers' band gap, but the issues related to the presence of Cd were not overcome.

6.1. Deposition techniques of alternative buffer layers

Beyond CBD, to efficiently grow buffer layers alternative to CdS several other deposition techniques have been used (Fig. 6), where sometimes the nature of the deposition itself is strongly affecting the final performance of the device. For instance, Zn(O,S) has been studied both deposited through CBD and Atomic Layer Deposition (ALD) as well as sputtering and High Vapor Transport Deposition (HVTD). While five years ago CBD seemed to be the best deposition route for this buffer layer, technology improved and nowadays ALD and HVTD equaled or even overcame the CBD [36,37,77,78]. In fact, the last two techniques, thanks to their working principles, guarantee more compact layers compared to CBD, where nucleation and growth processes compete into the solution and onto the sample's surface. This last feature leads necessarily to thicker layers in order to produce a continuous material and thus a true p-n junction. Particularly, both ALD and HVTD allow the

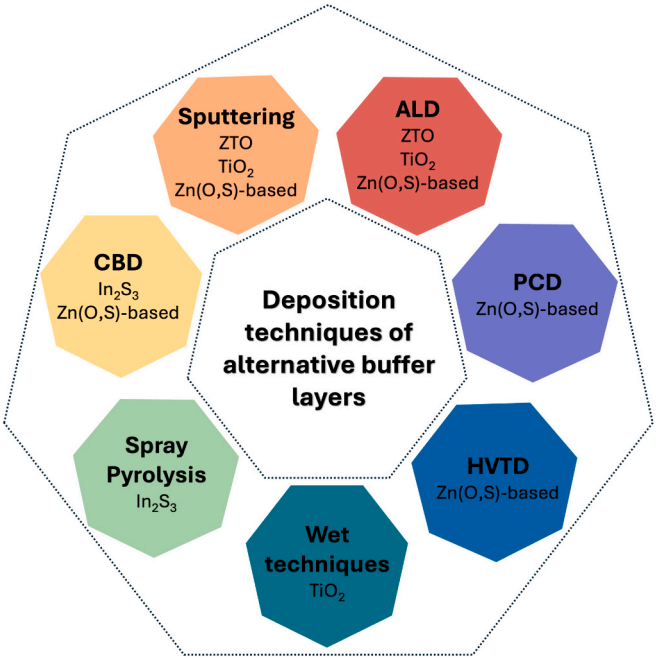

Fig. 6. Alternative buffer layers grouped by deposition techniques.

deposition of continuous and compact layers with a nanometric control, exploiting high-vacuum and low temperatures, reducing deposition times and excessive raw materials waste. As for $Zn_{1-x}Sn_xO$, it was deposited both through sputtering and ALD, but also in this case, the latter gave the most promising performances [14,15,34,35,79]. Despite both techniques involve high-vacuum and clean processes, sputtering employs high-energy sources which can degrade or alter the surface of the kesterite, while ALD again allows a softer procedure where the substrate with kesterite is preserved and in the meantime $Zn_{1-x}Sn_xO$ can be produced by fine and reproducible tuning of Zn and Sn. Recently, TiO_2 is emerging as buffer layer for kesterite PV cells and it has been also deposited through wet techniques as well as via ALD and with different crystalline phases [32,33,80–82]. In this case, the wet depositions are usually followed by an annealing step to convert titania in a crystalline rutile or anatase phase, while ALD guarantees an amorphous deposition of TiO_2 (apparently more useful for PV purposes). On the other hand, In_2S_3 was mainly deposited through wet techniques such as CBD or spray pyrolysis [26,40], which involve a great waste of precursors and often lead to layers of poor quality. However, due to the In low-abundance, the scientific community seems to be less interested in In_2S_3, thus it has not been furtherly studied and developed recently. Given that the most promising efficiencies (almost equaling CdS) have been reached with a relatively modern technology like ALD, it is possible to find its unique features as well as its advantages and disadvantages in the following section.

6.1.1. Buffer layer through ALD in kesterite solar cells

Atomic layer deposition (ALD) is a technique for depositing thin films that relies on the step-by-step and recurring introduction of gas/vapor phase species in a vacuum deposition chamber (Fig. 7). The gas components typically comprise at least one precursor and one co-reactant. Chemisorption reactions with self-limiting characteristics take place between these components and the functional groups existing on the substrate's surface. Specifically, in a two-step ALD process, the precursor reacts with the substrate's functional groups until saturation. Then, the co-reactant has the role to react with the chemisorbed precursor, removing the remaining ligands and restoring the original surface groups for the next cycle [83].

Thanks to the self-limiting nature of the reactions involved, ALD

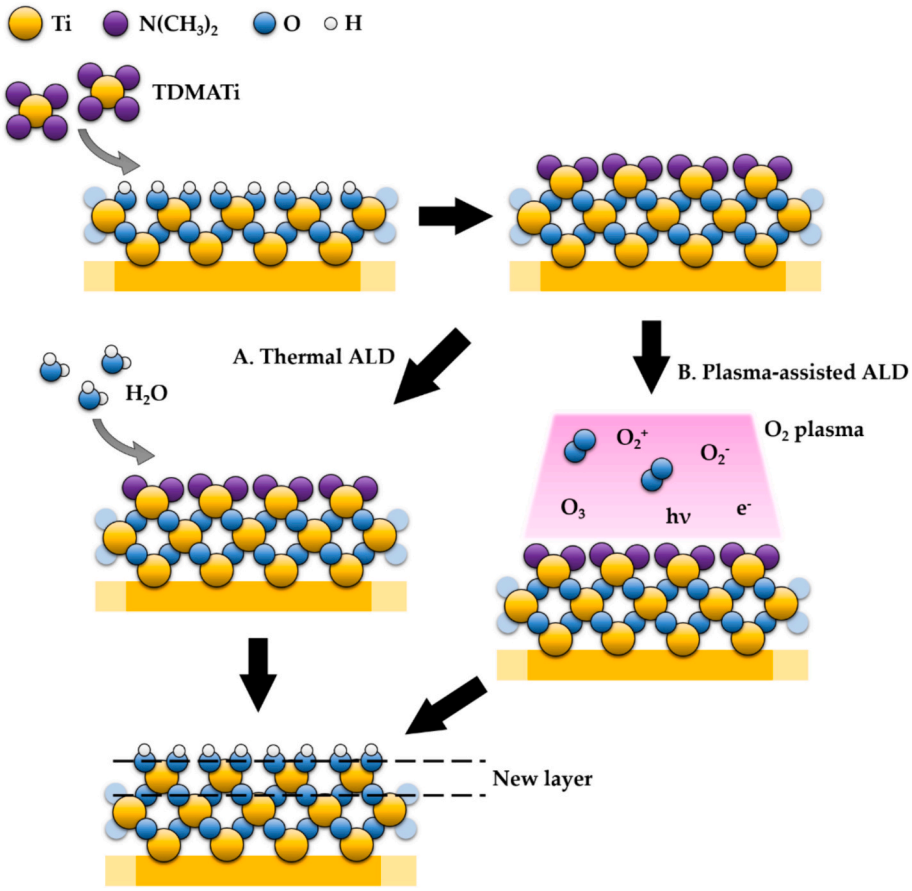

Fig. 7. (a) Thermal and (b) plasma-assisted ALD working principles.

enables for thickness control at atomic scale, excellent homogeneity, good control over the chemical composition of the material deposited and extremely good reproducibility [83,84]. Furthermore, as long as enough precursor/co-reactant is provided in order to reach saturation, ALD enables for conformal coverage into complex 3D substrates [85].

Application of ALD in the field of Cd-free kesterite solar cells is growing, taking advantage of all the above-mentioned aspects in order to improve the efficiency of the cells. For instance, Cui et al.[34] used an ultra-thin layer of ALD prepared Al_2O_3 in order to passivate surface defects at the grains of CZTS, improving the cell efficiency.

A huge part of the literature is reporting the use of ALD for the preparation of buffer layers for Cd-free kesterite solar cells. In this regard, ALD has the merit to allow for tuning of the material's composition, thanks to the possibility of combining different processes together [86,87].

This is the case for instance of several reports showing the ALD preparation of zinc-tin oxide (ZTO) buffer layers for Cd-free kesterite solar cells [14,15,27,35,88–90]. In that regard, the ZTO composition can be tuned by using different ratios between the Zn and Sn dosing in the ALD recipe, optimizing the buffer layer.

In a recent work instead, Tseberlidis et al.[32] used a TiO_2 buffer layer prepared by ALD. The choice was based on both theoretical work on the CZTS/TiO_2 junction and experimental reports using TiO_2 prepared by different techniques.

Therefore, the ALD of buffer layers for kesterite solar cells can offer several advantages, such as the precise thickness control (ensuring uniformity and consistency across the entire solar cell), conformal coating (meaning the buffer layer can coat complex and rough surfaces evenly), passivation of defects (reducing recombination losses, improving carrier transport, and enhancing the overall efficiency of the device), tuning band alignment (improving charge extraction and reducing losses at the heterojunction interface), enhanced stability (providing protection against environmental degradation and moisture ingress), compatibility with large-scale production. Overall, ALD of buffer layers offers a promising approach to enhance the efficiency, stability, and scalability of kesterite solar cells, thus advancing their commercial viability as a clean energy technology.

6.2. *Zn(O,S)-based buffer layers*

Zn(O,S) family buffer layers have been widely and deeply studied in the last decade with results ranging from good to bad, many times depending on the nature of the deposition technique used. Back into 2012, Barkhouse et al. [26] reported a detailed UPS study regarding the band alignment and the performance of several buffer layers alternative to CdS and among them we find ZnS deposited through CBD. From their study emerges that, when ZnS is coupled with CZTSSe, little current flow is registered, consistent with the large conduction band offset, leading to high resistance barrier to electron flow, unless the buffer layers were extremely thin (1–2 nm) allowing tunneling. In fact, ZnS shows a 1.1 eV spike at the interface, responsible of the considerable series resistance and the poor device performance. In 2014, Ericson and co-workers [91] reported their CZTS devices coupled with ALD-made Zn(O,S) (O:S ratio = 6:1) performing a promising 4.6% efficiency compared to a 7.3% efficiency of their CdS reference device. Parallelly, L. Grenet et al. [92], published their investigations on Cd-free CZTSSe based solar cells with a ZnS(O,OH) buffer layer deposited by CBD. The so-fabricated devices show power conversion efficiencies up to 5.8% after a prolonged light-soaking treatment. However, the efficiency is lower than their reference CdS-containing device (7.0%) related to a lower short circuit current. In 2015, Nguyen and co-workers [31] reported their solar devices based on CZTSSe monograins which registered efficiencies of $\eta = 4.5\%$

when coupled with 25 nm of ZnS made by CBD and compared to their CdS-containing reference device performing $\eta = 4.8\%$. Always in 2015, Steirer [93] described a double CBD strategy to deposit 20 nm of Zn(O,S) buffer layer by using either water or a mixture of water and DMSO as solvent. The corresponding devices, with architecture glass/Mo/CZTSe/CBD-ZnOS/i-ZnO/Al:ZnO, showed over 5% PCE when DMSO was used compared to PCE below 2% when only water was employed as solvent during CBD and this has been ascribed to alternate transport level that bypasses the large conduction band spike and allows the negative carriers generated under illumination to flow. In 2016, Hong et al. [28] studied the ALD of Zn(O,S) with many different O/(O + S) ratios. The highest efficiency of 2.75% was offered by the device containing the buffer layer with O/(O + S) = 0.67, compared to a 3.56% of a CdS-based CZTSSe solar cell. The optimized buffer layer was also employed on a Se-rich CZTSSe absorber and $\eta = 3.30\%$ was recorded (versus $\eta = 4.95\%$ of the CdS reference cell). Further improvement in performances from $\eta = 3.30\%$ to 4.68% was obtained by replacing H_2O with NH_4OH solution as oxygen source during of Zn(O,S) by ALD. This result indicates that specific growth conditions are of crucial importance to obtain a performance comparable to CdS using ALD-Zn(O,S) buffer layers.[28] In the same period, Neuschitzer and co-workers [77] have been able to correlate thiourea concentration during the CBD and light soaking to an improvement in the performances of CZTSSe/ZnS(O,OH) heterojunctions. Variations of the thiourea (TU) concentration in the CBD show a strong impact on device performance. A kink in illuminated J–V curves is observed for high TU concentrations (0.4 − 0.5 M) resulting in a barrier for photogenerated charges as expected from the high spike in the conduction band alignment, but the samples show a strong beneficial effect by light soaking. On the other hand, with [TU] = 0.3-0.35 M no distortions were observed but lower V_{OC} values are registered, and the samples are also less affected by light soaking. Overall, their optimized champion device exhibits $\eta = 6.5\%$ (when 0.4 M TU was used in the CBD) and after light soaking, to be compared with the $\eta = 6.9\%$ of the CdS reference device.[77] Also Hong et al. [94] reported on their ALD Zn(O,S) in 2017, with the upgrade of nitrogen doping in their oxygen rich buffer layer with beneficial effects. PCEs of 3% were obtained versus 4.5% of the CdS-based device. Always in 2017, Park et al. [95] reported on their 56 nm of CBD-made ZnS over CZTSSe with $\eta = 3.8\%$ versus their CZTSSe/CdS p-n junction performing $\eta = 5.2\%$. It is evident how the CBD conditions strongly influence the final device parameters and small differences in the procedures result in higher or lower efficiencies. However, in all cases ZnS was demonstrated to be a suitable candidate to substitute CdS with comparable results, when prepared through chemical routes. On the other hand, the same material has been produced also through sputtering (optimized at 30 nm) by Kim et al. [96] in 2014, but much lower performances were recorded ($\eta = 2.11\%$ versus $\eta = 4.97\%$ of the CdS-containing solar cell). Li and co-workers have been able to enhance the behavior of their CZTSe/Zn(O,S) devices by concentrated ammonium etching and soft annealing treatment [37]. In this way, ZnO and $Zn(OH)_2$ secondary phases were eliminated improving the hetero-junction quality. Moreover, thanks to the absence of high resistance i-ZnO window layer, and the use of anti-reflection coating, their solar cells showed small series resitance, high fill factor and $\eta = 7.2\%$ compared to $\eta = 8\%$ of the CdS-based cell. A different deposition technique was reported in 2019 by Zhang and co-workers [38]. Their novel ozone-assisted photochemical deposition (PCD) allowed them to produce working thin-film CZTS solar cells with ZnS or Zn(O,S) buffer layer. Despite the intriguing novelty, modest efficiencies were obtained for both the CZTS/ZnS and CZTS/Zn(O,S) p-n junctions (respectively $\eta = 1.9\%$ and $\eta = 3.0\%$) if compared to their CdS reference device relying on $\eta = 4.3\%$ and much higher J_{SC} and FF values. More recently, in 2021, Jeong and co-authors published interesting results regarding a facile $(NH_4)_2S$ solution treatment to improve the surface properties of their ALD-Zn(O,S) resulting in enhances device performances [36]. The cell efficiency of CZTSSe/Zn(O,S) drastically increased from 7.5% to 9.8% after 1 min of $(NH_4)_2S$ treatment resulting in removal of the native oxide layer, passivation with sulfur, reduction of the interfacial defects and recombination losses leading to higher V_{OC} and FF. The 9.8% record device has to be compared with the CdS-based device which shows $\eta = 10.1\%$, and in this way the authors experimentally demonstrate that Zn(O,S) could actually equal CdS as buffer layer in kesterite solar cells. Finally, in 2022, Delgado-Sanchez reported a Zn(O,S) buffer layer deposited though High Vapor Transport Deposition (HVTD) with which successfully tuned the band alignment between CZTSSe and the buffer layer [78]. The deep investigation involved different S/(S + O) ratios resulting in an optimized device when S/(S + O) range is 0.5–0.7, avoiding spike-like CBO, and leading to $\eta = 6.87\%$, $V_{OC} = 574$ mV, $J_{SC} = 20.3$ mA/cm^2 and 58.8% FF.

The extensive research, that has been conducted on Zn(O,S) family buffer layers for kesterite solar cells, has yielded mixed results influenced by the deposition techniques employed. Meanwhile the initial studies showed high resistance barriers due to a large conduction band offset, further investigations by different research groups explored various deposition methods and compositions, proving that Zn(O,S) can be a promising CdS substitute once the deposition conditions have been tuned to match the light absorber.

6.3. $Zn_{1-x}Sn_xO_y$ buffer layers

Among alternative buffer layers to CdS, ZTO has attracted great attention as it is based only on earth-abundant and non-toxic constituent elements,[88] has a large and tunable band gap, which makes possible to obtain good transparency and better energy band matching with kesterites [88], and is attractive for large scale production. Since 2012, this Cd-free buffer layer has shown promising results in CIGS-based solar cells, even surpassing the performance obtained with CdS [97,98], with efficiencies exceeding 18%[99]. The success of Cd-free CIGS solar cells has motivated researchers to use ZTO in kesterite devices as well. Since 2016, many results comparable to CdS have been achieved by synthesizing ZTO with different compositions and thicknesses on CZTS [15,34,100]. The main techniques used to growth high-quality ZTO are atomic layer deposition (ALD) and sputter deposition [15,34,89,101–103]. Thanks to its own advantages, such as excellent control of ZTO stoichiometry and thickness, atomic-scale precision, homogeneous deposition without damage to the kesterite surface [104], ALD-ZTO processes have attracted attention and, consequently, have been optimized by several groups. Moreover, this technique enables better cell-to-cell uniformity compared to CdS by CBD [88]. Li et al. [90] first reported the use of ALD-ZTO buffer layer in a CZTSSe device, demonstrating that the ZTO bandgap and the CBO of the ZTO/CZTSSe interface can be tuned and well controlled by varying proper Zn and Sn pulse ratio in the ALD process. They also studied the impact of the ZTO thickness on the device performances, showing that a too thin buffer layer may not fully cover the CZTSSe layer and, consequently, affect the p-n junction quality. On the contrary, when ZTO is too thick its resistance is very high, resulting in a FF decrease. In this work, with the optimized Sn/(Sn + Zn) pulse ratio equal to 0.167 and with a ZTO thickness of 50 nm, the champion CZTSSe/ZTO solar cell has achieved maximum efficiency of 8.60%, compared with 8.14% of the control device with CdS. Ericson et al. [100] demonstrated that by regulating the ALD-deposition temperature is possible to modify the band gap of the ZTO film and also the band alignment with the CZTS absorber. In this work the ALD process temperature was varied from 105 to 165 °C. Current-blocked solar cells were produced at 105 °C, the highest FF was obtained at 165 °C while the highest V_{OC} and efficiency of 9.0% were achieved at 145 °C. In the record device (in which 110 nm of MgF_2 antireflective coating, ARC, is inserted), ZTO grown at 145 °C has a thickness of 10 nm and a composition of Sn/(Sn + Zn) equal to 0.28. These PV results are better than the one of the control device with CdS (but without ARC), with efficiency of 7.2%. The authors also proved that the interface recombination at the p-n junction is significantly reduced, and the band alignment is improved for the ZTO samples compared to

the CdS-reference, suggesting that ZTO is very promising. Cui et al. [15] systematically investigated the structural and optical properties and optimized the stoichiometry and thickness of ALD-ZTO buffer layer to produce CZTS devices. The solar cells parameters proved the improvement in both J_{SC} and V_{OC}. They also studied the nanoscale structure of the devices, revealing the presence of an ultra-thin Zn(S,O) tunnel layer at the CZTS/ZTO junction which acts as hole barrier at the heterojunction interface and, thanks to the minor lattice mismatch at the CZTS/ Zn(S,O)/ZTO, reduces the defects at the heterointerface. Thanks to this ultra-thin Zn(S,O) layer and to a higher Na concentration in the ZTO based device, which provides passivation of defects, V_{OC} was increased up to 10%. In this way they have obtained a record efficiency of 9.3% using a 10 nm $Zn_{0.77}Sn_{0.23}O$ buffer layer and 110 nm of MgF_2, compared to 8.2% efficiency for the same cell but without ARC and to 6.9% efficiency for the control device with CdS and without ARC. One year later the same group for the first time inserted an ALD-Al_2O_3 passivation layer between CZTS and ZTO [34]. The authors demonstrated that Al_2O_3 and trimethylaluminum (TMA), which was used as Al_2O_3 precursor, lead to a variation of the CZTS surface chemical composition and a formation of a Na-rich and Cu-deficient nano-layer. This modification induced a band gap widening at the absorber surface, a reduction of defects recombination at the p-n junction and an improvement in V_{OC} and in PV performances, with a champion cell efficiency of 10.2%. Larsen et al. [103] optimized the energy band alignment at CZTS/ZTO junction, studying how the annealing conditions, the thermal history and the ordering treatment of the absorber impact on the band gap of the CZTS. For non-ordered CZTS the highest efficiency of 9.7% was achieved using ALD-ZTO (and with ARC). This is a great result, considering that the reference device with CdS (bur without ARC) has 7.5% efficiency. Gobbo et al. [35] have optimized ALD-ZTO composition and thicknesses. They have also demonstrated that the i-ZnO window layer deposited via sputtering, typically sandwiched between the buffer layer and the transparent contact in kesterite device architecture to prevent shunt, is not only redundant but also detrimental when coupled with high-homogeneous and compact ALD-ZTO. In fact, the conditions employed for the i-ZnO deposition process can alter the ZTO stoichiometry and properties, leading to an inter-layer which, due to its resistive nature, limits charge extraction. The authors find the best ZTO film with Sn/Zn ratio being 2:1 and with 30 nm thickness, achieving efficiency of 4.0% (without i-ZnO layer), slightly higher than the CZTS/CdS reference device (3.9%). Ahmad et al. [14] have shown that the ALD-ZTO buffer layer better the band alignment at the Ag-CZTSSe/ZTO junction. It is well known that Ag substitution in kesterite has a positive effect on the grain size growth of the absorber and consequently also on the device performance [105]. In this work the authors determined that 6% Ag substitution is the best performing. After properly tuning the composition and the thickness of ZTO, they proved that the best efficiency can be achieved with 10 nm ZTO with ALD pulse ratio of 5:1. The champion device with Ag-CZTSSe/ZTO exhibited 11.8% efficiency, higher if compared to both a CZTSSe/ZTO reference (10.9%) and to the standard device with Ag-CZTSSe/CdS (10.7%), confirming the relevant role of Ag and alternative buffer layer. To date this is the highest efficiency Cd-free kesterite solar cell (Fig. 8).

As mentioned above, also the sputtering technique allows to growth good-quality ZTO films and, thanks to its faster deposition rate and to its potential employment in low-cost mass production, has interested some research groups [89]. Grenet et al. [101] described the possibility of growing amorphous ZTO layers via sputtering of a single $Zn_{0.8}Sn_{0.2}O$ metal oxide target. A key parameter that had to be considered was the deposition power, which, if too high damages the absorber surface and reduces PV parameters, if too low results in a drastic increase in deposition time. To overcome these problems and conciliate the CZTS preservation and acceptable process time, a two-stages deposition with a first ultrathin low power layer and a second thicker higher power layer was performed. To further enhance the devices performances, the authors have also tested reactive sputtering with O_2, to obtain more transparent ZTO films, and with SF_6, to increase the conductivity of the buffer layer. The best results, achieving 5.2% efficiency, have been obtained with ZTO sputtered with O_2, surpassing the CZTS/CdS reference device (4.6%). In the paper the authors have also demonstrated that ZTO is more suitable for the sulfide kesterite rather than the Se-rich absorbers. Lee et al. have deposited ZTO through co-sputtering method [89]. They have studied and investigated band gap tuning of CZTSSe and ZTO in order to obtain an optimal CBO between them and to enhance V_{OC}. ZTO band gap was modulated by adjusting the Sn/(Zn + Sn) ratio and the deposition temperature. The buffer composition can be controlled by changing the power applied to each sputtering target. This band gap engineering led to a 11.22% efficiency (compared to CZTSSe/CdS reference device of 9.57%), thus resulting in the best data with sputtered ZTO. Zhang et al. have studied the effect of co-sputtered ZTO in pure CZTSe devices [79]. After the optimization of both ZTO composition, adjusted by varying the sputtering power ratio, and thickness, the buffer layer properties have also been improved via H_2-assisted reactive sputtering. It was demonstrated that the introduction of H_2 in the ZTO film implies an increase in carrier concentration and thus a reduction in ZTO resistance, leading to higher-performance devices. Thanks to these improvements, the highest efficiency obtained with CZTSe/ZTO solar cells is 5.08%, comparable with CZTSe/CdS reference device (5.86%). Lin et al. [106] first proposed an ultrathin CdS layer (10 nm), which acts as interface passivation layer and protection for CZTSSe surface, and 100 nm $Zn_{0.8}Sn_{0.2}O$ buffer layer (via co-sputtering) to limit Cd content and reduce interface recombination in flexible solar cells. With this device architecture it was possible to obtain high-quality interface and good band matching, achieving 9.3% efficiency, which is higher than that of the standard device with only CdS (8.5%). Recently, the same group has produced the first flexible CZTSSe solar cells with

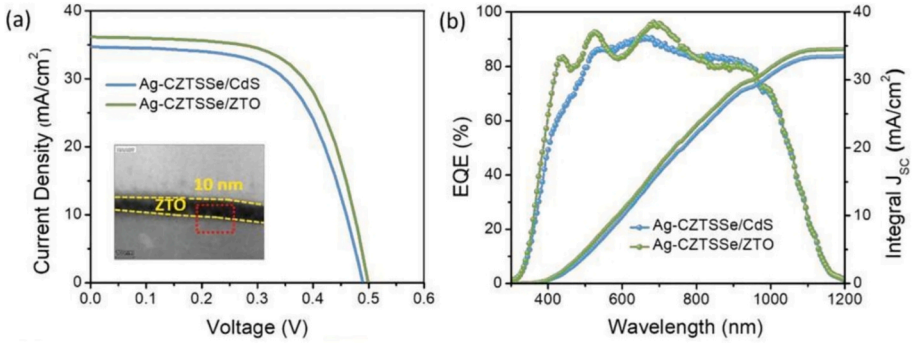

Fig. 8. (a) J-V curve of the highest efficiency Cd-free kesterite solar cell (Ag-CZTSSe/ZTO junction) compared to its reference CdS-based device. (b) EQE and Integral J_{SC} of the highest efficiency Cd-free kesterite solar cell (Ag-CZTSSe/ZTO junction) compared to its reference CdS-based device. (Reproduced Under the Terms of CC BY License, Copyright 2023, Advanced Science, Wiley, [14]).

only ZTO deposited via co-sputtering, finally leading to a device efficiency of 8.7%, which is the maximum value reported for Cd-free flexible kesterite devices [107]. These results are due to a low roughness ZTO, which is fundamental to improve junction interface quality, enhance carrier transport capability and reduce the scattering of incident photons.

Therefore, ZTO buffer layer has been proved to be a valid alternative to CdS since it has shown comparable performance to the conventional device architecture. Various synthesis methods, including ALD and sputter deposition, have been utilized to fabricate high-quality ZTO layers, showing promising results in achieving high-performance kesterite solar cells. Moreover, the integration of ZTO buffer layers in flexible solar cells has also been explored, resulting in significant efficiency enhancements, highlighting the potential of ZTO as a key component in next-generation Cd-free kesterite solar cell technology.

6.4. In_2S_3-based buffer layers

Among the suitable alternatives to CdS to be coupled with kesterites, we find also In_2S_3. This material has been studied in the early stages of the research on this topic and immediately gave promising results, even comparable to CdS. However, the use of a rare and expensive element like indium (indicating also difficulties in a possible industrial scale-up) and the further improvements achieved by the CZTSSe/CdS junction, somehow hindered the investigations and turned the attention of the research community towards other materials. Nevertheless, some of the best efficiencies with alternative buffer layers have been achieved by using In_2S_3, so it deserves to be mentioned and commented in this review [40,76,108,109]. The crystalline forms and phases of In_2S_3 have been deeply investigated and it seems that the β-In_2S_3 phase leads to higher performances when used in kesterite thin film solar cells, thanks to its stability, optical and electronic properties. Moreover, at the interface with CZTSSe an interdiffusion gradient is formed which seems to carry beneficial effects for the device behavior [41,108,110]. Exciting results were recorded in 2012 when In_2S_3 was deposited through CBD by Barkhouse and co-workers [26], $\eta = 7.19\%$ was obtained for CZTSSe/In_2S_3 compared to $\eta = 7.75\%$ of the CdS reference device. The efficiency was furtherly improved to $\eta = 7.59\%$ by using MgF_2 anti-reflective coating (ARC). Always depositing In_2S_3 through CBD, Hiroi et al. [111] in 2012 reported their results, with $\eta = 6.3\%$ for CZTS/In_2S_3 heterojunction, even though no CdS-reference device was reported, but only the comparison with the other novel heterojunction proposed between CZTS and ZnO:B (made by metal-organic chemical vapor deposition-MOCVD) relying on $\eta = 5.85\%$. A few years later, Jiang et al. studied and reported on the CZTS interface doping by In_2S_3 induced by the post-heating treatment after the CBD deposition, which allowed $\eta = 6.9\%$ compared to the $\eta = 8.1\%$ of their CZTS/CdS reference device [39,41]. In the same period also a promising chemically spray pyrolyzed (CSP) version of In_2S_3 was proposed by Khadka [40] coupled with low band gap kesterite (CZTSe) achieving $\eta = 5.74\%$, but no reference device was reported and compared there. Other works have been published, between 2014 and 2016, involving In_2S_3 but it was used together with CdS in structures where both the materials were stacked, resulting in a beneficial effect for the band alignment, even though cadmium was still present and an expensive element like indium was added in the meantime [75,76]. However, since 2016 the kesterite/In_2S_3 research slows down with other emerging buffer layers taking the stage: ZnSnO and Zn(O,S) mainly. Nevertheless, given the stuck in the efficiency improvement for kesterite solar cells, in the last few years a reprise of the topic is being pushed from the theoretical point of view, mainly through SCAPS simulations, where In_2S_3 is still presented as one of the best candidates to be coupled with kesterites [112–114].

So, despite its initial success, the rarity and expense of indium, along with the superior performance of CZTSSe/CdS junctions, diverted research attention towards other materials. However, some of the highest efficiencies with alternative buffer layers have been achieved using In_2S_3, particularly the β-In_2S_3 phase, known for its stability and beneficial interdiffusion effects at the CZTSSe interface, which should be taken as a positive example for the design of cheaper buffer layers.

6.5. TiO_2 as buffer layer

In the plethora of TiO_2 applications we can find also photovoltaics [115–120]. In fact, titania is being intensively used in perovskites as well as in dye sensitized solar cells (DSSC) as hole transport layer due to its features. In particular, it shows very good conductive properties, it is produced through relatively low-cost chemicals and, depending on its thickness, it exhibits also high values of transmittance thus limiting parasitic absorptions. However, it is barely reported in combination with chalcogenides in the generation of a p-n junction for photovoltaic purposes [115,121,122]. In recent times, apparently the interest of the kesterite research community towards this material has increased and several works have been published regarding theory, modelling, simulations and calculations, indicating TiO_2 as a suitable candidate to replace CdS in kesterite thin-film solar cells. Simulations made from Bencherif and coworkers [72] seem to justify TiO_2 use above CdS thanks to a possible ~5% V_{OC} gain. In the same work, the simulated device would be able to both overcome fill factor (FF) and efficiency (η) current CZTS/CdS limitations, reaching values respectively of FF ~ 86% and η ~ 15%. Few years ago, also Nisika [123,124] reported on CZTS/TiO_2 experimental/simulated heterojunctions, proving through UPS and XPS measurements that in this case a favorable spike-like effect in the band alignment leads to an offset CB of 0.17 eV. The same authors reported also on the TiO_2 conductivity related to oxygen vacancies which strongly affects the charge extraction, enhancing it when lower values of oxygen are present [123,124].

Despite the good and encouraging theoretical results achieved, very little evidence has been recorded on the topic, especially if compared to the above-described buffer layers. Back in 2015, Demopoulos et al. [80] developed an unconventional and sophisticated route to grow nanocrystallites of CZTS on nanorod-arrays of titania (TiO_2-NA), producing in this way the first working solar cell based on CZTS/TiO_2 junction. The device architecture was in superstrate configuration (TCO/TiO_2/interlayer/CZTS-NA/top-contact) and showed modest characteristics with V_{OC} ~ 180 mV and J_{SC} ~ 3.3 mA/cm^2. However, the optimization of their synthetic procedure and device production lead to better performances in 2019, with η ~ 1%, V_{OC} ~ 400 mV and J_{SC} ~ 6.6 mA/cm^2, this time interposing Al_2O_3 between CZTS and TiO_2-NA in a sort of p-i-n junction [81]. In the last few years, other works have been published coupling CZTS with titania but still inserting a thin CdS layer in between and leading to efficiencies <1%[82,125]. In 2021, Dwivedi and coworkers [126] published their superstrate solar cell produced with facile and chemically deposited commercial TiO_2 and CZTS but reaching again modest device parameters like $\eta = 0.87\%$, $V_{OC} = 400$ mV, $J_{SC} = 4.7$ mA/cm^2. In 2022, Wang and coworkers [33] recorded outstanding results with their Ag-substituted low band-gap kesterite in superstrate configuration with a sputtered layer of TiO_2. Despite the use of Ag in their (Cu,Ag)$_2$ZnSn(S,Se)$_4$ kesterite and of an expensive layer of PTB7 and Au contacts, they have been able to reach $\eta = 9.7\%$, $V_{OC} = 0.49$ V, $J_{SC} = 31.4$ mA/cm^2 and FF = 63%. In 2023, Tseberlidis and coworkers [32] reported their substrate configuration device with CZTS/TiO2 heterojunction showing 3.01% with a J_{SC} of 16 mA/cm^2 and V_{OC} 460 mV and relying on the simplest architecture possible Mo/CZTS/TiO_2/AZO/Al. The authors used ALD to deposit amorphous titania directly over a sputtered CZTS and compared their novel device with a CdS-based reference one showing $\eta = 4\%$. They experimentally demonstrate that TiO_2 can be a good candidate to substitute CdS and that comparable cell parameters can be achieved by using ALD-TiO_2. Interestingly, the best results have been achieved after 1 h of light-soaking on the final device, supporting the observations regarding the oxygen vacancies tuning described by Nisika et al.[123], and suggesting that this heterojunction could work even better in normal operating conditions. Recent

unpublished results of Tseberlidis and co-workers, reported in this review, regard the stability of the same CZTS/TiO_2 devices, where improvements in solar cell parameters were achieved after 18 months of ageing and always after 1 h of light soaking, which allowed to furtherly increase the efficiency of the device to $\eta = 3.71\%$ (Table 1, last entry).

Summing up, TiO_2 is a well-known material in PV, due to its transparency and cost-effectiveness, and lately it has been also explored in combination with chalcogenides. Experimental efforts have shown promising results, with CZTS/TiO_2 heterojunctions demonstrating favorable band alignments and charge extraction properties. Although experimental evidence remains limited compared to other buffer layers, stability studies have shown promising results, indicating improvements in device parameters over time. Overall, these findings suggest that TiO_2 could be revolutionary in kesterite solar cells, with opportunities for further optimization and enhancement of device performance.

7. Conclusions

In thin film kesterite solar cell technology, CdS is commonly used as the n-type partner (buffer layer) but, beyond its toxicity, it shows a nonoptimal band alignment with kesterites (regardless of their band gap) and exhibits parasitic absorption at low wavelengths due to its bandgap. Several efforts have been made in the last decade, to replace CdS with a suitable, Cd-free, both environmentally and economically sustainable buffer layer, and many times with successful results allowing not only to equal, but also to overcome in few cases the performances of the corresponding CdS-based reference devices. Several architectures have been optimized and employed, depending on the buffer layer chosen to substitute CdS (Fig. 9). The record devices for each alternative buffer layer are summarized in Table 1 in comparison with their corresponding CdS-based device. In Fig. 10 are reported the efficiencies of all the devices cited in this review featuring alternative buffer layers and representing the milestones of the research on this hot topic.

Zn(O,S) family buffer layers for kesterite solar cells have been extensively studied, and have yielded mixed results strongly influenced by the employed deposition technique. Initially it showed high resistance barriers due to a large conduction band offset. However, further investigations adopting various deposition methods and compositions, proved that Zn(O,S) can be a suitable CdS substitute when the deposition conditions have been tuned to match the light absorber. On the other hand, ZTO buffer layer has been proved to be a valid alternative to CdS since it has shown comparable performance to the conventional device architecture containing CdS. Different growth methods, and among them ALD and sputtering, have been employed to fabricate high-quality ZTO layers, registering promising results and achieving high-performance kesterite PV devices. In addition to this, ZTO has been successfully employed also in flexible solar cells carrying significant efficiency enhancements, thus highlighting the potential of ZTO as a key component in next-generation Cd-free kesterite solar cells. As for In_2S_3, despite its initial success, the low abundance and cost of indium together with lower performances compared to kesterite/CdS junctions, diminished the interest towards this material. TiO_2 is one of the emerging most

Table 1
Kesterite record devices divided by alternative buffer layers used and compared to the corresponding CdS-based reference devices where available.

Absorber	E_g (eV)	Architecture	BL	BL deposition	BL thickness (nm)	V_{OC} (mV)	J_{SC} (mA/cm^2)	FF (%)	η (%)	Area (cm^2)	Year	Ref.
CZTSe	1.02	substrate	Zn(O,S) CdS	CBD CBD	25 NA	358 388	33.5 35.9	60 58	7.2[a] 8.0	0.345	2017	[37]
CZTSSe	1.09	substrate	Zn(O,S) CdS	ALD CBD	20 20	496 482	35.6 36.4	56 58	9.8 10.1	0.3	2021	[36]
CZTS	NA	substrate	Zn(O,S) CdS	ALD CBD	33 50	482 652	17.2 17.5	55.5 63.8	4.6 7.3	NA	2014	[91]
CZTSe	NA	substrate	ZnSnO CdS	Sputtering CBD	10 50	370 376	24.39 32.72	56.28 47.63	5.08 5.86	NA	2021	[79]
CZTSSe[b]	1.08	substrate	ZnSnO CdS	ALD CBD	10 40	498 490	36.28 34.83	66.53 62.96	11.8 10.7	0.135	2023	[14]
CZTS	1.5	substrate	ZnSnO[a, e] CdS	ALD CBD	10 50	736 652	21.0 16.5	65.8 6.9	10.2 6.9	0.224	2019	[15,34]
CZTSe	1.08	substrate	In_2S_3 CdS	CSP -	100 -	431 -	28.3 -	47.1 -	5.74 -	0.1 -	2015 -	[40] -
CZTSSe	1.2	substrate	In_2S_3 CdS	CBD CBD	< 50 nm < 50 nm	424 465	32.3 27.1	55 62	7.59 7.75[a]	NA	2012	[26]
CZTS	1.4	substrate	In_2S_3 CdS	CBD CBD	90 90	621 705	20 18	54.5 63.2	6.9 8.1	0.05	2016	[39,41]
CZTSe	- -	- -	TiO_2 CdS	- -	- -	- -	- -	- -	- -	- -	- -	- -
CZTSSe[b]	1.19	superstrate	TiO_2 CdS	Sputtering -	20 nm -	490 -	31.4 -	63 -	9.7 -	0.03 -	2022 -	[33] -
CZTS	1.58	substrate	TiO_2 TiO_2 CdS	ALD ALD CBD	20 nm 20 nm 70 nm	465 476 555	16.5 17.7 16.1	39.1 44.0 59.7	3.01[c] 3.71[c, d] 4.14	0.11	2023	[32] *New Results*[f] [32]

[a] with anti-reflection coating (ARC).
[b] silver refined kesterite $(Cu,Ag)_2ZnSn(S,Se)_4$
[c] after 1 h light soaking
[d] after 18 months of ageing
[e] with Al_2O_3 interlayer; BL = Buffer Layer
[f] The authors of this review report here the updated efficiencies after ageing process of their CZTS/TiO_2 device already reported in reference [32] by the same authors.

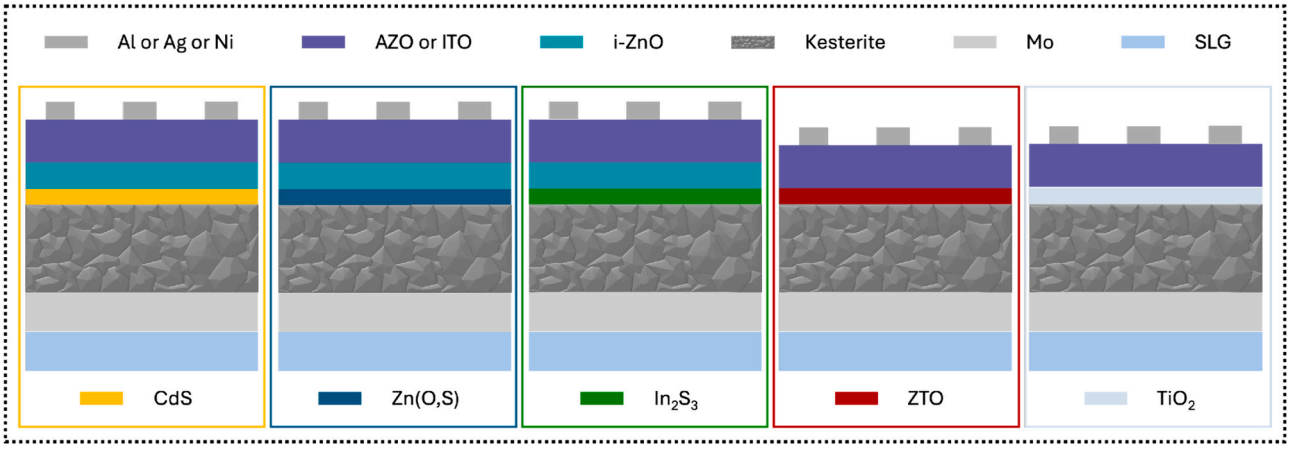

Fig. 9. Device architecture of the champion devices for each alternative buffer layer reported.

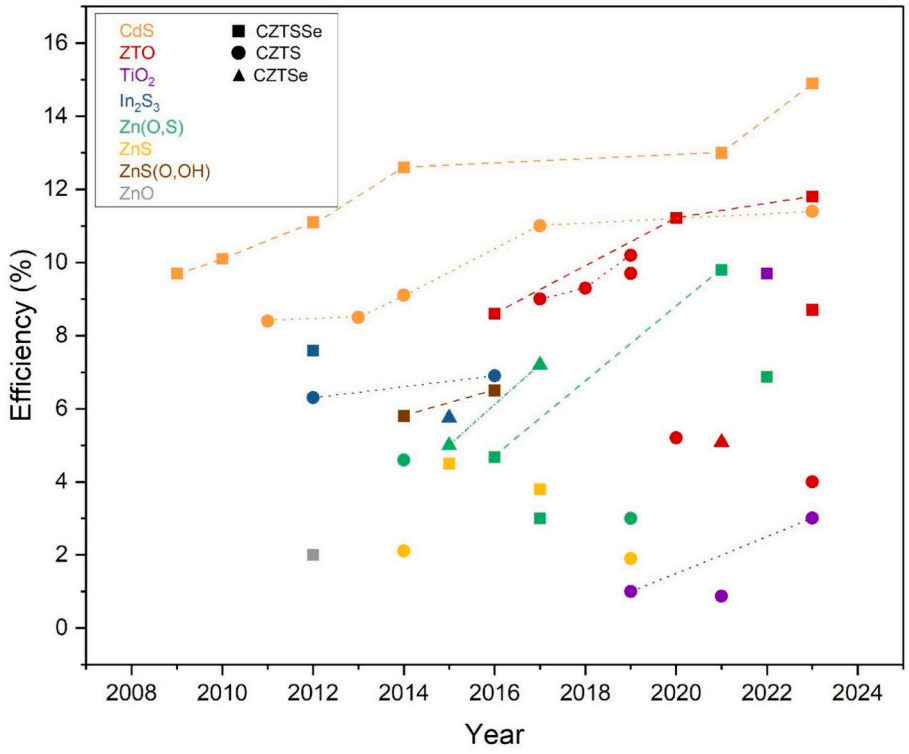

Fig. 10. Power conversion efficiencies recorded with different Cd-free buffer layers for CZTSe, CZTSSe, CZTS thin-film solar cells (each colored spot corresponds to a work cited and described in the main text).

promising candidates to substitute CdS. It is well known thanks to its transparency and cost-effectiveness and recent findings about its combination with chalcogenide absorbers gave promising results. Both theoretical and experimental investigations demonstrated favorable band alignments and charge extraction properties and, despite the still low efficiencies compared to other alternative buffer layers, stability studies indicate improvements in device parameters over time. These findings suggest that TiO_2 could be revolutionary in kesterite solar cells, with opportunities for further optimization and enhancement of device performance.

What undoubtedly emerges is that, among all the reported deposition techniques, the ALD of buffer layers for kesterite solar cells can offer several advantages, such as the precise thickness control (ensuring uniformity and consistency across the entire solar cell), conformal coating (meaning the buffer layer can coat complex and rough surfaces evenly), passivation of defects (reducing recombination losses, improving carrier transport, and enhancing the overall efficiency of the device), tuning band alignment (improving charge extraction and reducing losses at the heterojunction interface), enhanced stability (providing protection against environmental degradation and moisture ingress), compatibility with large-scale production. Overall, ALD of buffer layers offers a promising approach to enhance the efficiency, stability, and scalability of kesterite solar cells, thus advancing their commercial viability as a clean energy technology. In conclusion, in this review we summarized the efforts and the improvements recorded by the scientific community working on alternative buffer layers for kesterites in the last ten years, with the aim to supply a landmark useful to design future experiments in a more efficient way and to push forward the related research activities, in order to fully overcome CdS limitations and to promote thin-film kesterite devices to higher performances.

Therefore, in the future scenario of the "Terawatt Era", PV will play a lead role in many applications, including PIPV, such as "wearables", BIPV and VIPV, where light-weight thin-film technologies are mandatory, and Cd-free kesterite thin-film solar cells can emerge as the main candidate for an environmental-friendly energy production.

Funding

This study has been supported by "nuovi Concetti, mAteriali e tecnologie per l'iNtegrazione del fotoVoltAico negli edifici in uno scenario di generazione diffuSa" [CANVAS] project, funded by the Italian Ministry of the Environment and the Energy Security, through the Research Fund for the Italian Electrical System (type-A call, published on G.U.R.I. n. 192 on 18-08-2022).

This work has been supported by [MUSA] – Multilayered Urban Sustainability Action – project, funded by the European Union – NextGenerationEU, under the National Recovery and Resilience Plan (NRRP) Mission 4 Component 2 Investment Line 1.5: Strenghtening of research structures and creation of R&D "innovation ecosystems", set up of "territorial leaders in R&D".

CRediT authorship contribution statement

G. Tseberlidis: Writing – review & editing, Writing – original draft, Visualization, Supervision, Conceptualization. **C. Gobbo:** Writing – review & editing, Writing – original draft, Visualization. **V. Trifiletti:** Writing – review & editing, Writing – original draft, Visualization. **V. Di Palma:** Writing – review & editing, Writing – original draft, Visualization. **S. Binetti:** Writing – review & editing, Supervision, Funding acquisition.

Declaration of competing interest

None.

Data availability

No data was used for the research described in the article.

References

[1] M. He, C. Yan, J. Li, M.P. Suryawanshi, J. Kim, M.A. Green, X. Hao, Kesterite solar cells: insights into current strategies and challenges, Adv. Sci. 8 (2021) 2004313, https://doi.org/10.1002/advs.202004313.

[2] M.A. Green, E.D. Dunlop, M. Yoshita, N. Kopidakis, K. Bothe, G. Siefer, X. Hao, Solar cell efficiency tables (version 62), Prog. Photovolt. Res. Appl. 31 (2023) 651–663, https://doi.org/10.1002/pip.3726.

[3] Z. Su, G. Liang, P. Fan, J. Luo, Z. Zheng, Z. Xie, W. Wang, S. Chen, J. Hu, Y. Wei, C. Yan, J. Huang, X. Hao, F. Liu, Device Postannealing enabling over 12% efficient solution-processed Cu2ZnSnS4 solar cells with Cd2+ substitution, Adv. Mater. 32 (2020) 2000121, https://doi.org/10.1002/adma.202000121.

[4] Z. Yu, C. Li, S. Chen, Z. Zheng, P. Fan, Y. Li, M. Tan, C. Yan, X. Zhang, Z. Su, G. Liang, Unveiling the Selenization reaction mechanisms in ambient air-processed highly efficient Kesterite solar cells, Adv. Energy Mater. 13 (2023) 2300521, https://doi.org/10.1002/aenm.202300521.

[5] G.-X. Liang, C.-H. Li, J. Zhao, Y. Fu, Z.-X. Yu, Z.-H. Zheng, Z.-H. Su, P. Fan, X.-H. Zhang, J.-T. Luo, L. Ding, S. Chen, Self-powered broadband kesterite photodetector with ultrahigh specific detectivity for weak light applications, SusMat 3 (2023) 682–696, https://doi.org/10.1002/sus2.160.

[6] G. Liang, Z. Li, M. Ishaq, Z. Zheng, Z. Su, H. Ma, X. Zhang, P. Fan, S. Chen, Charge separation enhancement enables record photocurrent density in Cu2ZnSn(S,Se)4 photocathodes for efficient solar hydrogen production, Adv. Energy Mater. 13 (2023) 2300215, https://doi.org/10.1002/aenm.202300215.

[7] Y. Zhao, S. Chen, M. Ishaq, M. Cathelinaud, C. Yan, H. Ma, P. Fan, X. Zhang, Z. Su, G. Liang, Controllable double gradient bandgap strategy enables high efficiency solution-processed Kesterite solar cells, Adv. Funct. Mater. 34 (2024) 2311992, https://doi.org/10.1002/adfm.202311992.

[8] P. Fan, J. Lin, J. Hu, Z. Yu, Y. Zhao, S. Chen, Z. Zheng, J. Luo, G. Liang, Z. Su, Over 10% efficient Cu2CdSnS4 solar cells fabricated from optimized sulfurization, Adv. Funct. Mater. 32 (2022) 2207470, https://doi.org/10.1002/adfm.202207470.

[9] Y. Li, Z. Wang, Y. Zhao, D. Luo, X. Zhang, J. Zhao, Z. Su, S. Chen, G. Liang, Potassium doping for grain boundary passivation and defect suppression enables highly-efficient kesterite solar cells, Chin. Chem. Lett. (2024) 109468, https://doi.org/10.1016/j.cclet.2023.109468.

[10] Y. Zhao, Z. Yu, J. Hu, Z. Zheng, H. Ma, K. Sun, X. Hao, G. Liang, P. Fan, X. Zhang, Z. Su, Over 12% efficient kesterite solar cell via back interface engineering, J. Energy Chemistry 75 (2022) 321–329, https://doi.org/10.1016/j.jechem.2022.08.031.

[11] F. Liu, Q. Zeng, J. Li, X. Hao, A. Ho-Baillie, J. Tang, M.A. Green, Emerging inorganic compound thin film photovoltaic materials: Progress, challenges and strategies, Mater. Today 41 (2020) 120–142, https://doi.org/10.1016/j.mattod.2020.09.002.

[12] W. Wang, M.T. Winkler, O. Gunawan, T. Gokmen, T.K. Todorov, Y. Zhu, D. B. Mitzi, Device characteristics of CZTSSe thin-film solar cells with 12.6% efficiency, Adv. Energy Mater. 4 (2014) 1301465, https://doi.org/10.1002/aenm.201301465.

[13] C. Yan, J. Huang, K. Sun, S. Johnston, Y. Zhang, H. Sun, A. Pu, M. He, F. Liu, K. Eder, L. Yang, J.M. Cairney, N.J. Ekins-Daukes, Z. Hameiri, J.A. Stride, S. Chen, M.A. Green, X. Hao, Cu2ZnSnS4 solar cells with over 10% power conversion efficiency enabled by heterojunction heat treatment, Nat. Energy 3 (2018) 764–772, https://doi.org/10.1038/s41560-018-0206-0.

[14] N. Ahmad, Y. Zhao, F. Ye, J. Zhao, S. Chen, Z. Zheng, P. Fan, C. Yan, Y. Li, Z. Su, X. Zhang, G. Liang, Cadmium-free Kesterite thin-film solar cells with high efficiency approaching 12%, Adv. Sci. 10 (2023) 2302869, https://doi.org/10.1002/advs.202302869.

[15] X. Cui, K. Sun, J. Huang, C.-Y. Lee, C. Yan, H. Sun, Y. Zhang, F. Liu, Md. A. Hossain, Y. Zakaria, L.H. Wong, M. Green, B. Hoex, X. Hao, Enhanced heterojunction Interface quality to achieve 9.3% efficient cd-free Cu2ZnSnS4 solar cells using atomic layer deposition ZnSnO buffer layer, Chem. Mater. 30 (2018) 7860–7871, https://doi.org/10.1021/acs.chemmater.8b03398.

[16] H. Wei, Y. Li, C. Cui, X. Wang, Z. Shao, S. Pang, G. Cui, Defect suppression for high-efficiency kesterite CZTSSe solar cells: advances and prospects, Chem. Eng. J. 462 (2023) 142121, https://doi.org/10.1016/j.cej.2023.142121.

[17] A. Nagoya, R. Asahi, G. Kresse, First-principles study of Cu2ZnSnS4 and the related band offsets for photovoltaic applications, J. Phys. Condens. Matter 23 (2011) 404203, https://doi.org/10.1088/0953-8984/23/40/404203.

[18] A. Santoni, F. Biccari, C. Malerba, M. Valentini, R. Chierchia, A. Mittiga, Valence band offset at the CdS/Cu2ZnSnS4 interface probed by x-ray photoelectron spectroscopy, J. Phys. D. Appl. Phys. 46 (2013) 175101, https://doi.org/10.1088/0022-3727/46/17/175101.

[19] M. Courel, J.A. Andrade-Arvizu, O. Vigil-Galán, Towards a CdS/Cu2ZnSnS4 solar cell efficiency improvement: a theoretical approach, Appl. Phys. Lett. 105 (2014) 233501, https://doi.org/10.1063/1.4903826.

[20] M. Bär, B.-A. Schubert, B. Marsen, R.G. Wilks, S. Pookpanratana, M. Blum, S. Krause, T. Unold, W. Yang, L. Weinhardt, C. Heske, H.-W. Schock, Cliff-like conduction band offset and KCN-induced recombination barrier enhancement at the CdS/Cu2ZnSnS4 thin-film solar cell heterojunction, Appl. Phys. Lett. 99 (2011) 222105, https://doi.org/10.1063/1.3663327.

[21] K. Pal, P. Singh, A. Bhaduri, K.B. Thapa, Current challenges and future prospects for a highly efficient (>20%) kesterite CZTS solar cell: a review, Sol. Energy Mater. Sol. Cells 196 (2019) 138–156, https://doi.org/10.1016/j.solmat.2019.03.001.

[22] R. Haight, A. Barkhouse, O. Gunawan, B. Shin, M. Copel, M. Hopstaken, D. B. Mitzi, Band alignment at the Cu2ZnSn(SxSe1−x)4/CdS interface, Appl. Phys. Lett. 98 (2011) 253502, https://doi.org/10.1063/1.3600776.

[23] C. Yan, F. Liu, N. Song, B.K. Ng, J.A. Stride, A. Tadich, X. Hao, Band alignments of different buffer layers (CdS, Zn(O,S), and In2S3) on Cu2ZnSnS4, Appl. Phys. Lett. 104 (2014) 173901, https://doi.org/10.1063/1.4873715.

[24] C. Platzer-Björkman, N. Barreau, M. Bär, L. Choubrac, L. Grenet, J. Heo, T. Kubart, A. Mittiga, Y. Sanchez, J. Scragg, S. Sinha, M. Valentini, Back and front contacts in kesterite solar cells: state-of-the-art and open questions, J. Phys. Energy 1 (2019) 044005, https://doi.org/10.1088/2515-7655/ab3708.

[25] A. Wang, M. He, M.A. Green, K. Sun, X. Hao, A critical review on the Progress of Kesterite solar cells: current strategies and insights, Adv. Energy Mater. 13 (2023) 2203046, https://doi.org/10.1002/aenm.202203046.

[26] D.A.R. Barkhouse, R. Haight, N. Sakai, H. Hiroi, H. Sugimoto, D.B. Mitzi, Cd-free buffer layer materials on Cu2ZnSn(SxSe1−x)4: band alignments with ZnO, ZnS, and In2S3, Appl. Phys. Lett. 100 (2012) 193904, https://doi.org/10.1063/1.4714737.

[27] S. Sinha, D.K. Nandi, S.-H. Kim, J. Heo, Atomic-layer-deposited buffer layers for thin film solar cells using earth-abundant absorber materials: a review, Sol. Energy Mater. Sol. Cells 176 (2018) 49–68, https://doi.org/10.1016/j.solmat.2017.09.044.

[28] H.K. Hong, I.Y. Kim, S.W. Shin, G.Y. Song, J.Y. Cho, M.G. Gang, J.C. Shin, J. H. Kim, J. Heo, Atomic layer deposited zinc oxysulfide n-type buffer layers for Cu2ZnSn(S,Se)4 thin film solar cells, Sol. Energy Mater. Sol. Cells 155 (2016) 43–50, https://doi.org/10.1016/j.solmat.2016.04.054.

[29] H.S. Nugroho, G. Refantero, N.L.W. Septiani, M. Iqbal, S. Marno, H. Abdullah, E. C. Prima, B. Yuliarto Nugraha, A progress review on the modification of CZTS (e)-based thin-film solar cells, J. Ind. Eng. Chem. 105 (2022) 83–110, https://doi.org/10.1016/j.jiec.2021.09.010.

[30] L.-Y. Lin, Y. Qiu, Y. Zhang, H. Zhang, Analysis of Effect of Zn(O,S) Buffer Layer Properties on CZTS Solar Cell Performance Using AMPS*, Chin. Phys. Lett. 33 (2016) 107801, https://doi.org/10.1088/0256-307X/33/10/107801.

[31] M. Nguyen, K. Ernits, K.F. Tai, C.F. Ng, S.S. Pramana, W.A. Sasangka, S. K. Batabyal, T. Holopainen, D. Meissner, A. Neisser, L.H. Wong, ZnS buffer layer for Cu2ZnSn(SSe)4 monograin layer solar cell, Sol. Energy 111 (2015) 344–349, https://doi.org/10.1016/j.solener.2014.11.006.

[32] G. Tseberlidis, V. Di Palma, V. Trifiletti, L. Frioni, M. Valentini, C. Malerba, A. Mittiga, M. Acciarri, S.O. Binetti, Titania as buffer layer for cd-free Kesterite solar cells, ACS Mater Lett 5 (2023) 219–224, https://doi.org/10.1021/acsmaterialslett.2c00933.
[33] Z. Wang, Y. Wang, N. Taghipour, L. Peng, G. Konstantatos, Ag-refined Kesterite in superstrate solar cell configuration with 9.7% power conversion efficiency, Adv. Funct. Mater. 32 (2022) 2205948, https://doi.org/10.1002/adfm.202205948.
[34] X. Cui, K. Sun, J. Huang, J.S. Yun, C.-Y. Lee, C. Yan, H. Sun, Y. Zhang, C. Xue, K. Eder, L. Yang, J.M. Cairney, J. Seidel, N.J. Ekins-Daukes, M. Green, B. Hoex, X. Hao, Cd-free Cu2ZnSnS4 solar cell with an efficiency greater than 10% enabled by Al2O3 passivation layers, energy, Environ. Sci. 12 (2019) 2751–2764, https://doi.org/10.1039/C9EE01726G.
[35] C. Gobbo, V. Di Palma, V. Trifiletti, C. Malerba, M. Valentini, I. Matacena, S. Daliento, S. Binetti, M. Acciarri, G. Tseberlidis, Effect of the ZnSnO/AZO Interface on the charge extraction in cd-free Kesterite solar cells, Energies (Basel) 16 (2023), https://doi.org/10.3390/en16104137.
[36] H. Jeong, R. Nandi, J.Y. Cho, P.S. Pawar, H.S. Lee, K.E. Neerugatti, J.H. Kim, J. Heo, CZTSSe/Zn(O,S) heterojunction solar cells with 9.82% efficiency enabled via (NH4)2S treatment of absorber layer, Prog. Photovolt. Res. Appl. 29 (2021) 1057–1067, https://doi.org/10.1002/pip.3439.
[37] J. Li, X. Liu, W. Liu, L. Wu, B. Ge, S. Lin, S. Gao, Z. Zhou, F. Liu, Y. Sun, J. Ao, H. Zhu, Y. Mai, Y. Zhang, Restraining the Band Fluctuation of CBD-Zn(O,S) Layer: Modifying the Hetero-Junction Interface for High Performance Cu2ZnSnSe4 Solar Cells With Cd-Free Buffer Layer, Sol. RRL 1 (2017) 1700075, https://doi.org/10.1002/solr.201700075.
[38] J. Zhang, J. Feng, Y. Feng, J. Liao, S. Xue, L. Shao, G. Liang, Fabrication of Zn(O, S) thin films by ozone assisted photochemical deposition and its potential applications as buffer layers in kesterite-based thin film solar cells, Thin Solid Films 670 (2019) 80–85, https://doi.org/10.1016/j.tsf.2018.12.002.
[39] F. Jiang, S. Ikeda, Z. Tang, T. Minemoto, W. Septina, T. Harada, M. Matsumura, Impact of alloying duration of an electrodeposited cu/Sn/Zn metallic stack on properties of Cu2ZnSnS4 absorbers for thin-film solar cells, Prog. Photovolt. Res. Appl. 23 (2015) 1884–1895, https://doi.org/10.1002/pip.2638.
[40] D.B. Khadka, S. Kim, J. Kim, A nonvacuum approach for fabrication of Cu2ZnSnSe4/In2S3 thin film solar cell and optoelectronic characterization, J. Phys. Chem. C 119 (2015) 12226–12235, https://doi.org/10.1021/acs.jpcc.5b03193.
[41] F. Jiang, C. Ozaki, T. Gunawan, Z. Harada, T. Tang, Y. Minemoto, S. Ikeda Nose, Effect of indium doping on surface Optoelectrical properties of Cu2ZnSnS4 Photoabsorber and interfacial/photovoltaic performance of cadmium free In2S3/Cu2ZnSnS4 heterojunction thin film solar cell, Chem. Mater. 28 (2016) 3283–3291, https://doi.org/10.1021/acs.chemmater.5b04984.
[42] X. Cui, K. Sun, J. Huang, H. Sun, A. Wang, X. Yuan, M. Green, B. Hoex, X. Hao, Low-temperature plasma-enhanced atomic layer deposition of ZnMgO for efficient CZTS solar cells, ACS Mater Lett 5 (2023) 1456–1465, https://doi.org/10.1021/acsmaterialslett.2c01203.
[43] S. Mohammadnejad, Z. Mollaaghaei Bahnamiri, S. Enayati Maklavani, Enhancement of the performance of kesterite thin-film solar cells using dual absorber and ZnMgO buffer layers, Superlattice. Microst. 144 (2020) 106587, https://doi.org/10.1016/j.spmi.2020.106587.
[44] G. Tseberlidis, V. Trifiletti, E. Vitiello, A.H. Husien, L. Frioni, M. Da Lisca, J. Alvarez, M. Acciarri, S.O. Binetti, Band-gap tuning induced by germanium introduction in solution-processed Kesterite thin films, ACS Omega 7 (2022) 23445–23456, https://doi.org/10.1021/acsomega.2c01786.
[45] U. Saha, Md.K. Alam, Boosting the efficiency of single junction kesterite solar cell using ag mixed Cu2ZnSnS4 active layer, RSC Adv. 8 (2018) 4905–4913, https://doi.org/10.1039/C7RA12352C.
[46] S.R. Kodigala, Thin Film Solar Cells from Earth Abundant Materials Growth and Characterization of Cu2(ZnSn)(SSe)4 Thin Films and their Solar Cells, 1st ed., Elsevier, 2013.
[47] S.R. Kodigala, Cu(In1-xGax)Se2 Based Thin Film Solar Cells, 1st ed., Academic Press, 2010.
[48] H. Katagiri, N. Sasaguchi, S. Hando, S. Hoshino, J. Ohashi, T. Yokota, Preparation and evaluation of Cu2ZnSnS4 thin films by sulfurization of EB evaporated precursors, Sol. Energy Mater. Sol. Cells 49 (1997) 407–414, https://doi.org/10.1016/S0927-0248(97)00119-0.
[49] Z. Wang, Y. Wang, G. Konstantatos, Highly efficient, ultrathin, cd-free kesterite solar cells in superstrate configuration enabled by band level tuning via ag incorporation, Nano Energy 94 (2022) 106898, https://doi.org/10.1016/j.nanoen.2021.106898.
[50] F. Assunta Pisu, P.C. Ricci, S. Porcu, C.M. Carbonaro, D. Chiriu, Degradation of CdS yellow and Orange pigments: a preventive characterization of the process through pump–probe, reflectance, X-ray Diffract. Raman Spectr. Materials 15 (2022), https://doi.org/10.3390/ma15165533.
[51] D. Payno, S. Kazim, M. Salado, S. Ahmad, Sulfurization temperature effects on crystallization and performance of superstrate CZTS solar cells, Sol. Energy 224 (2021) 1136–1143, https://doi.org/10.1016/j.solener.2021.06.038.
[52] G. Tseberlidis, A. Hasan Husien, S. Riva, L. Frioni, A. Le Donne, M. Acciarri, S. Binetti, Semi-transparent Cu2ZnSnS4 solar cells by drop-casting of sol-gel ink, Sol. Energy 224 (2021) 134–141, https://doi.org/10.1016/j.solener.2021.05.073.
[53] M. Espindola-Rodriguez, D. Sylla, Y. Sánchez, F. Oliva, S. Grini, M. Neuschitzer, L. Vines, V. Izquierdo-Roca, E. Saucedo, M. Placidi, Bifacial Kesterite solar cells on FTO substrates, ACS Sustain. Chem. Eng. 5 (2017) 11516–11524, https://doi.org/10.1021/acssuschemeng.7b02797.
[54] M.S. Aida, S. Hariech, Cadmium sulfide thin films by chemical Bath deposition technique, in: S.J. Ikhmayies (Ed.), Advances in Energy Materials, Springer International Publishing, Cham, 2020, pp. 49–75, https://doi.org/10.1007/978-3-030-50108-2_3.
[55] G. Tseberlidis, V. Trifiletti, A. Le Donne, L. Frioni, M. Acciarri, S. Binetti, Kesterite solar-cells by drop-casting of inorganic sol–gel inks, Sol. Energy 208 (2020) 532–538, https://doi.org/10.1016/j.solener.2020.07.093.
[56] X. Li, D. Zhuang, N. Zhang, M. Zhao, X. Yu, P. Liu, Y. Wei, G. Ren, Achieving 11.95% efficient Cu2ZnSnSe4 solar cells fabricated by sputtering a cu–Zn–Sn–se quaternary compound target with a selenization process, J. Mater. Chem. A Mater. 7 (2019) 9948–9957, https://doi.org/10.1039/C9TA00385A.
[57] S. Gao, Z. Jiang, L. Wu, J. Ao, Y. Zeng, Y. Sun, Y. Zhang, Interfaces of high-efficiency kesterite Cu2ZnSnS(e)4 thin film solar cells*, Chin. Phys. B 27 (2018) 018803, https://doi.org/10.1088/1674-1056/27/1/018803.
[58] K. Nisika, M. Kaur, Progress and prospects of CZTSSe/CdS interface engineering to combat high open-circuit voltage deficit of kesterite photovoltaics: a critical review, J. Mater. Chem. A Mater. 8 (2020) 21547–21584, https://doi.org/10.1039/D0TA06450E.
[59] M. Kangsabanik, R.N. Gayen, A comprehensive review on the recent strategy of cation substitution in CZTS(se) thin films to achieve highly efficient Kesterite solar cells, Solar RRL 2300670 (2023), https://doi.org/10.1002/solr.202300670.
[60] N. Saini, N.M. Martin, J.K. Larsen, A. Hultqvist, T. Törndahl, C. Platzer-Björkman, Record 1.1 V open-circuit voltage for Cu2ZnGeS4-based thin-film solar cells using atomic layer deposition Zn1-x Sn x O y buffer layers, Sol. RRL 6 (2022) 2100837, https://doi.org/10.1002/solr.202100837.
[61] S. Oueslati, M. Grossberg, M. Kauk-Kuusik, V. Mikli, K. Ernits, D. Meissner, J. Krustok, Effect of germanium incorporation on the properties of kesterite Cu2ZnSn(S,Se)4 monograins, Thin Solid Films 669 (2019) 315–320, https://doi.org/10.1016/j.tsf.2018.11.020.
[62] M. Ritzer, S. Schönherr, P. Schöppe, W. Wisniewski, S. Giraldo, G. Gurieva, A. Johannes, C.T. Plass, K. Ritter, G. Martínez-Criado, S. Schorr, E. Saucedo, C. Ronning, C.S. Schnohr, On the germanium incorporation in Cu2ZnSnSe4 Kesterite solar cells boosting their efficiency, ACS Appl. Energy Mater. 3 (2020) 558–564, https://doi.org/10.1021/acsaem.9b01784.
[63] S.A. Vanalakar, P.S. Patil, J.H. Kim, Recent advances in synthesis of Cu2FeSnS4 materials for solar cell applications: a review, Sol. Energy Mater. Sol. Cells 182 (2018) 204–219, https://doi.org/10.1016/j.solmat.2018.03.021.
[64] Y. Sun, X. Li, W. Qiao, L. Wu, S. Gao, H. Li, F. Liu, J. Ao, Y. Zhang, A promising photovoltaic material Cu2MnSn(S,Se)4: Film growth and its application in solar cell, Sol. Energy Mater. Sol. Cells 219 (2021) 110788, https://doi.org/10.1016/j.solmat.2020.110788.
[65] V. Trifiletti, G. Tseberlidis, M. Colombo, A. Spinardi, S. Luong, M. Danilson, M. Grossberg, O. Fenwick, S. Binetti, Growth and characterization of Cu2Zn1−xFexSnS4 thin films for photovoltaic applications, Materials 13 (2020), https://doi.org/10.3390/ma13061471.
[66] V. Trifiletti, L. Frioni, G. Tseberlidis, E. Vitiello, M. Danilson, M. Grossberg, M. Acciarri, S. Binetti, S. Marchionna, Manganese-substituted kesterite thin-films for earth-abundant photovoltaic applications, Sol. Energy Mater. Sol. Cells 254 (2023) 112247, https://doi.org/10.1016/j.solmat.2023.112247.
[67] N. Saini, J.K. Larsen, K. Lindgren, A. Fazi, C. Platzer-Björkman, Bandgap engineered Cu2ZnGexSn1−xS4 solar cells using an adhesive TiN back contact layer, J. Alloys Compd. 880 (2021) 160478, https://doi.org/10.1016/j.jallcom.2021.160478.
[68] M. Gansukh, Z. Li, M.E. Rodriguez, S. Engberg, F.M.A. Martinho, S.L. Mariño, E. Stamate, J. Schou, O. Hansen, S. Canulescu, Energy band alignment at the heterointerface between CdS and ag-alloyed CZTS, Sci. Rep. 10 (2020) 18388, https://doi.org/10.1038/s41598-020-73828-0.
[69] S. Rondiya, Y. Jadhav, M. Nasane, S. Jadkar, N.Y. Dzade, Interface structure and band alignment of CZTS/CdS heterojunction: an experimental and first-principles DFT investigation, Materials 12 (2019), https://doi.org/10.3390/ma12244040.
[70] S. Rondiya, A. Rokade, P. Sharma, M. Chaudhary, A. Funde, Y. Jadhav, S. Haram, H. Pathan, S. Jadkar, CZTS/CdS: interface properties and band alignment study towards photovoltaic applications, J. Mater. Sci. Mater. Electron. 29 (2018) 4201–4210, https://doi.org/10.1007/s10854-017-8365-5.
[71] T. Nagai, T. Shimamura, K. Tanigawa, Y. Iwamoto, H. Hamada, N. Ohta, S. Kim, H. Tampo, H. Shibata, K. Matsubara, S. Niki, N. Terada, Band alignment of the CdS/Cu2Zn(Sn1–xGex)Se4 Heterointerface and electronic properties at the Cu2Zn(Sn1–xGex)Se4 surface: x = 0, 0.2, and 0.4, ACS Appl. Mater. Interfaces 11 (2019) 4637–4648, https://doi.org/10.1021/acsami.8b19200.
[72] H. Bencherif, L. Dehimi, N. Mahsar, E. Kouriche, F. Pezzimenti, Modeling and optimization of CZTS kesterite solar cells using TiO2 as efficient electron transport layer, Mater. Sci. Eng. B 276 (2022) 115574, https://doi.org/10.1016/j.mseb.2021.115574.
[73] R. Uwe Hertwig, Investigation of Interface and Device Properties in cd-Free CIGS Thin Film Solar Cells with Vapor and Plasma Deposited ZnMgO Buffer Layers, 1989.
[74] K. Sun, C. Yan, F. Liu, J. Huang, F. Zhou, J.A. Stride, M. Green, X. Hao, Over 9% efficient Kesterite Cu2ZnSnS4 solar cell fabricated by using Zn1–xCdxS buffer layer, Adv. Energy Mater. 6 (2016) 1600046, https://doi.org/10.1002/aenm.201600046.
[75] C. Yan, F. Liu, K. Sun, N. Song, J.A. Stride, F. Zhou, X. Hao, M. Green, Boosting the efficiency of pure sulfide CZTS solar cells using the in/cd-based hybrid buffers, Sol. Energy Mater. Sol. Cells 144 (2016) 700–706, https://doi.org/10.1016/j.solmat.2015.10.019.
[76] J. Kim, H. Hiroi, T.K. Todorov, O. Gunawan, M. Kuwahara, T. Gokmen, D. Nair, M. Hopstaken, B. Shin, Y.S. Lee, W. Wang, H. Sugimoto, D.B. Mitzi, High

efficiency Cu2ZnSn(S,Se)4 solar cells by applying a double In2S3/CdS emitter, Adv. Mater. 26 (2014) 7427–7431, https://doi.org/10.1002/adma.201402373.
[77] M. Neuschitzer, K. Lienau, M. Guc, L.C. Barrio, S. Haass, J.M. Prieto, Y. Sanchez, M. Espindola-Rodriguez, Y. Romanyuk, A. Perez-Rodriguez, V. Izquierdo-Roca, E. Saucedo, Towards high performance Cd-free CZTSe solar cells with a ZnS(O, OH) buffer layer: the influence of thiourea concentration on chemical bath deposition, J. Phys. D. Appl. Phys. 49 (2016) 125602, https://doi.org/10.1088/0022-3727/49/12/125602.
[78] J.-M. Delgado-Sanchez, I. Lillo-Bravo, J.A. López-Álvarez, E. Pérez-Aparicio, Zn (O,S) Buffer Layer Deposited by High Vapor Transport Deposition for Controlling Band Alignment of Cu2ZnSn(SxSe1−x)4 Thin-Film Solar Cell Heterojunction, Sol. RRL 6 (2022) 2200818, https://doi.org/10.1002/solr.202200818.
[79] S. Zhang, J. Wu, H. Guo, Y. Sun, Z. Zhou, Y. Zhang, Optimization of Zn1–xSnxO buffer layer for application in CZTSe solar cells with H2-assisted reactive sputtering, Phys. Status Solidi A 218 (2021) 2100585, https://doi.org/10.1002/pssa.202100585.
[80] Z. Wang, G.P. Demopoulos, Growth of Cu2ZnSnS4 Nanocrystallites on TiO2 Nanorod arrays as novel extremely thin absorber solar cell structure via the successive-ion-layer-adsorption-reaction method, ACS Appl. Mater. Interfaces 7 (2015) 22888–22897, https://doi.org/10.1021/acsami.5b05732.
[81] Z. Wang, N. Brodusch, R. Gauvin, G.P. Demopoulos, New Insight into Sulfurized and Selenized Kesterite–Titania Nanostructures for CdS-free and HTM-free Photovoltaic and Voltage-Modulated Photodetecting Applications, ACS Sustain. Chem. Eng. 7 (2019) 15093–15101, https://doi.org/10.1021/acssuschemeng.9b03814.
[82] V.V. Satale, S.V. Bhat, Superstrate type CZTS solar cell with all solution processed functional layers at low temperature, Sol. Energy 208 (2020) 220–226, https://doi.org/10.1016/j.solener.2020.07.055.
[83] S.M. George, Atomic layer deposition: an overview, Chem. Rev. 110 (2010) 111–131, https://doi.org/10.1021/cr900056b.
[84] A. Pandiyan, V. Di Palma, V. Kyriakou, W.M.M. Kessels, M. Creatore, M.C.M. van de Sanden, M.N. Tsampas, Enhancing the Electrocatalytic activity of redox stable perovskite fuel electrodes in solid oxide cells by atomic layer-deposited Pt nanoparticles, ACS Sustain. Chem. Eng. 8 (2020) 12646–12654, https://doi.org/10.1021/acssuschemeng.0c04274.
[85] V. Cremers, R.L. Puurunen, J. Dendooven, Conformality in atomic layer deposition: current status overview of analysis and modelling, Appl. Phys. Rev. 6 (2019) 021302, https://doi.org/10.1063/1.5060967.
[86] S.K. Kim, G.-J. Choi, C.S. Hwang, Controlling the composition of doped materials by ALD: a case study for Al-doped TiO2 films, Electrochem. Solid-State Lett. 11 (2008) G27, https://doi.org/10.1149/1.2909768.
[87] V. Di Palma, G. Zafeiropoulos, T. Goldsweer, W.M.M. Kessels, M.C.M. van de Sanden, M. Creatore, M.N. Tsampas, Atomic layer deposition of cobalt phosphate thin films for the oxygen evolution reaction, Electrochem. Commun. 98 (2019) 73–77, https://doi.org/10.1016/j.elecom.2018.11.021.
[88] J.Y. Cho, J.S. Jang, V.C. Karade, R. Nandi, P.S. Pawar, T.-J. Seok, W. Moon, T. J. Park, J.H. Kim, J. Heo, Atomic-layer-deposited ZnSnO buffer layers for kesterite solar cells: impact of Zn/(Zn+Sn) ratio on device performance, J. Alloys Compd. 895 (2022) 162651, https://doi.org/10.1016/j.jallcom.2021.162651.
[89] J. Lee, T. Enkhbat, G. Han, M.H. Sharif, E. Enkhbayar, H. Yoo, J.H. Kim, S. Kim, J. Kim, Over 11 % efficient eco-friendly kesterite solar cell: Effects of S-enriched surface of Cu2ZnSn(S,Se)4 absorber and band gap controlled (Zn,Sn)O buffer, Nano Energy 78 (2020) 105206, https://doi.org/10.1016/j.nanoen.2020.105206.
[90] X. Li, Z. Su, S. Venkataraj, S.K. Batabyal, L.H. Wong, 8.6% efficiency CZTSSe solar cell with atomic layer deposited Zn-Sn-O buffer layer, Sol. Energy Mater. Sol. Cells 157 (2016) 101–107, https://doi.org/10.1016/j.solmat.2016.05.032.
[91] T. Ericson, J.J. Scragg, A. Hultqvist, J.T. Wätjen, P. Szaniawski, T. Törndahl, C. Platzer-Björkman, Zn(O, S) buffer layers and thickness variations of CdS buffer for cu $_{2}$ZnSnS$_{4}$ solar cells, IEEE J. Photovolt. 4 (2014) 465–469, https://doi.org/10.1109/JPHOTOV.2013.2283058.
[92] L. Grenet, P. Grondin, K. Coumert, N. Karst, F. Emieux, F. Roux, R. Fillon, G. Altamura, H. Fournier, P. Faucherand, S. Perraud, Experimental evidence of light soaking effect in Cd-free Cu2ZnSn(S,Se)4-based solar cells, Thin Solid Films 564 (2014) 375–378, https://doi.org/10.1016/j.tsf.2014.05.033.
[93] K.X. Steirer, R.L. Garris, J.V. Li, M.J. Dzara, P.F. Ndione, K. Ramanathan, I. Repins, G. Teeter, C.L. Perkins, Co-solvent enhanced zinc oxysulfide buffer layers in Kesterite copper zinc tin selenide solar cells, Phys. Chem. Chem. Phys. 17 (2015) 15355–15364, https://doi.org/10.1039/C5CP01607J.
[94] H.K. Hong, G.Y. Song, H.J. Shim, J.H. Kim, J. Heo, Recovery of rectifying behavior in Cu2ZnSn(S,Se)4/Zn(O,S) thin-film solar cells by in-situ nitrogen doping of buffer layers, Sol. Energy 145 (2017) 20–26, https://doi.org/10.1016/j.solener.2016.09.042.
[95] J.Y. Park, R.B.V. Chalapathy, A.C. Lokhande, C.W. Hong, J.H. Kim, Fabrication of earth abundant Cu2ZnSnSSe4 (CZTSSe) thin film solar cells with cadmium free zinc sulfide (ZnS) buffer layers, J. Alloys Compd. 695 (2017) 2652–2660, https://doi.org/10.1016/j.jallcom.2016.11.178.
[96] J. Kim, C. Park, S.M. Pawar, A.I. Inamdar, Y. Jo, J. Han, J. Hong, Y.S. Park, D.-Y. Kim, W. Jung, H. Kim, H. Im, Optimization of sputtered ZnS buffer for Cu2ZnSnS4 thin film solar cells, Thin Solid Films 566 (2014) 88–92, https://doi.org/10.1016/j.tsf.2014.07.024.
[97] A. Hultqvist, C. Platzer-Björkman, U. Zimmermann, M. Edoff, T. Törndahl, Growth kinetics, properties, performance, and stability of atomic layer deposition Zn–Sn–O buffer layers for Cu(In,Ga)Se2 solar cells, Prog. Photovolt. Res. Appl. 20 (2012) 883–891, https://doi.org/10.1002/pip.1153.
[98] J. Lindahl, J.T. Wätjen, A. Hultqvist, T. Ericson, M. Edoff, T. Törndahl, The effect of Zn1−xSnxOy buffer layer thickness in 18.0% efficient Cd-free Cu(In,Ga)Se2 solar cells, in: Progress in Photovoltaics: Research and Applications 21, 2013, pp. 1588–1597, https://doi.org/10.1002/pip.2239.
[99] J. Lindahl, U. Zimmermann, P. Szaniawski, T. Törndahl, A. Hultqvist, P. Salomé, C. Platzer-Björkman, M. Edoff, Inline Cu(In,Ga)Se$_{2}$ co-evaporation for high-efficiency solar cells and modules, IEEE J. Photovolt. 3 (2013) 1100–1105, https://doi.org/10.1109/JPHOTOV.2013.2256232.
[100] T. Ericson, F. Larsson, T. Törndahl, C. Frisk, J. Larsen, V. Kosyak, C. Hägglund, S. Li, C. Platzer-Björkman, Zinc-tin-oxide buffer layer and low temperature post annealing resulting in a 9.0% efficient cd-free Cu2ZnSnS4 solar cell, Sol. RRL 1 (2017) 1700001, https://doi.org/10.1002/solr.201700001.
[101] L. Grenet, F. Emieux, J. Andrade-Arvizu, E. De Vito, G. Lorin, Y. Sánchez, E. Saucedo, F. Roux, Sputtered ZnSnO buffer layers for Kesterite solar cells, ACS Appl. Energy Mater. 3 (2020) 1883–1891, https://doi.org/10.1021/acsaem.9b02329.
[102] R.A. Mereu, A. Le Donne, S. Trabattoni, M. Acciarri, S. Binetti, Comparative study on structural, morphological and optical properties of Zn2SnO4 thin films prepared by r.f. sputtering using Zn and Sn metal targets and ZnO–SnO2 ceramic target, J. Alloys Compd. 626 (2015) 112–117, https://doi.org/10.1016/j.jallcom.2014.11.150.
[103] J.K. Larsen, F. Larsson, T. Törndahl, N. Saini, L. Riekehr, Y. Ren, A. Biswal, D. Hauschild, L. Weinhardt, C. Heske, C. Platzer-Björkman, Cadmium free Cu2ZnSnS4 solar cells with 9.7% efficiency, Adv. Energy Mater. 9 (2019) 1900439, https://doi.org/10.1002/aenm.201900439.
[104] Md.A. Hossain, K.T. Khoo, X. Cui, G.K. Poduval, T. Zhang, X. Li, W.M. Li, B. Hoex, Atomic layer deposition enabling higher efficiency solar cells: a review, Nano, Mater. Sci. 2 (2020) 204–226, https://doi.org/10.1016/j.nanoms.2019.10.001.
[105] S. Giraldo, Z. Jehl, M. Placidi, V. Izquierdo-Roca, A. Pérez-Rodríguez, E. Saucedo, Progress and perspectives of thin film Kesterite photovoltaic technology: a critical review, Adv. Mater. 31 (2019) 1806692, https://doi.org/10.1002/adma.201806692.
[106] B. Lin, Q. Sun, C. Zhang, H. Deng, W. Xie, J. Tang, Q. Zheng, J. Wu, H. Zhou, S. Cheng, 9.3% efficient flexible Cu2ZnSn(S,Se)4 solar cells with high-quality interfaces via ultrathin CdS and Zn0.8Sn0.2O buffer layers, Energ. Technol. 10 (2022) 2200571, https://doi.org/10.1002/ente.202200571.
[107] B. Lin, Q. Sun, C. Zhang, H. Deng, Y. Li, W. Xie, Y. Li, Q. Zheng, J. Wu, S. Cheng, Efficient cd-free flexible CZTSSe solar cells with quality interfaces by using the Zn1–xSnxO buffer layer, ACS Appl. Energy Mater. 6 (2023) 1037–1045, https://doi.org/10.1021/acsaem.2c03541.
[108] S. Siol, T.P. Dhakal, G.S. Gudavalli, P.P. Rajbhandari, C. DeHart, L.L. Baranowski, A. Zakutayev, Combinatorial reactive sputtering of In2S3 as an alternative contact layer for thin film solar cells, ACS Appl. Mater. Interfaces 8 (2016) 14004–14011, https://doi.org/10.1021/acsami.6b02213.
[109] V.G. Rajeshmon, N. Poornima, C. Sudha Kartha, K.P. Vijayakumar, Modification of the optoelectronic properties of sprayed In2S3 thin films by indium diffusion for application as buffer layer in CZTS based solar cell, J. Alloys Compd. 553 (2013) 239–244, https://doi.org/10.1016/j.jallcom.2012.11.106.
[110] L. Bhira, H. Essaidi, S. Belgacem, G. Couturier, J. Salardenne, N. Barreaux, J. C. Bernede, Structural and photoelectrical properties of sprayed β-In2S3 thin films, Phys. Status Solidi A 181 (2000) 427–435, https://doi.org/10.1002/1521-396X(200010)181:2<427::AID-PSSA427>3.0.CO;2-P.
[111] IEEE Electron Devices Society., Institute of Electrical and Electronics Engineers, Photovoltaic Specialists Conference (PVSC), 2012 38th IEEE, 2012.
[112] D. Alam, S. Deb, F. Faiza, Comparative study of CZTS solar cell with different buffers and BSF layer, in: 2022 4th International Conference on Sustainable Technologies for Industry 4.0 (STI), 2022, pp. 1–5, https://doi.org/10.1109/STI56238.2022.10103278.
[113] B. Eghbalifar, H. Izadneshan, G. Solookinejad, L. Separdar, Investigating In2S3 as the buffer layer in CZTSSe solar cells using simulation and experimental approaches, Solid State Commun. 343 (2022) 114654, https://doi.org/10.1016/j.ssc.2022.114654.
[114] S. Tripathi, B. Kumar, D.K. Dwivedi, Numerical simulation of non-toxic In2S3/SnS2 buffer layer to enhance CZTS solar cells efficiency by optimizing device parameters, Optik (Stuttg) 227 (2021) 166087, https://doi.org/10.1016/j.ijleo.2020.166087.
[115] A.S. Mathur, P.P. Singh, S. Upadhyay, N. Yadav, K.S. Singh, D. Singh, B.P. Singh, Role of absorber and buffer layer thickness on Cu2O/TiO2 heterojunction solar cells, Sol. Energy 233 (2022) 287–291, https://doi.org/10.1016/j.solener.2022.01.047.
[116] P. Nunez, M.H. Richter, B.D. Piercy, C.W. Roske, M. Cabán-Acevedo, M.D. Losego, S.J. Konezny, D.J. Fermin, S. Hu, B.S. Brunschwig, N.S. Lewis, Characterization of electronic transport through amorphous TiO2 produced by atomic layer deposition, J. Phys. Chem. C 123 (2019) 20116–20129, https://doi.org/10.1021/acs.jpcc.9b04434.
[117] T. Su, Y. Yang, Y. Na, R. Fan, L. Li, L. Wei, B. Yang, W. Cao, An insight into the role of oxygen vacancy in hydrogenated TiO2 nanocrystals in the performance of dye-sensitized solar cells, ACS Appl. Mater. Interfaces 7 (2015) 3754–3763, https://doi.org/10.1021/am5085447.
[118] O.E. Dagdeviren, D. Glass, R. Sapienza, E. Cortés, S.A. Maier, P. Parkin, P. Grütter, R. Quesada-Cabrera, The effect of Photoinduced surface oxygen vacancies on the charge carrier dynamics in TiO2 films, Nano Lett. 21 (2021) 8348–8354, https://doi.org/10.1021/acs.nanolett.1c02853.
[119] X. Zhang, H. Tian, X. Wang, G. Xue, Z. Tian, J. Zhang, S. Yuan, T. Yu, Z. Zou, The role of oxygen vacancy-Ti3+ states on TiO2 nanotubes' surface in dye-sensitized

solar cells, Mater. Lett. 100 (2013) 51–53, https://doi.org/10.1016/j.matlet.2013.02.116.
[120] W. Hsu, C.M. Sutter-Fella, M. Hettick, L. Cheng, S. Chan, Y. Chen, Y. Zeng, M. Zheng, H.-P. Wang, C.-C. Chiang, A. Javey, Electron-selective TiO2 contact for Cu(In,Ga)Se2 solar cells, Sci. Rep. 5 (2015) 16028, https://doi.org/10.1038/srep16028.
[121] A. Chihi, M.F. Boujmil, B. Bessais, Investigation on the performance of CIGS/TiO2 heterojunction using SCAPS software for highly efficient solar cells, J. Electron. Mater. 46 (2017) 5270–5277, https://doi.org/10.1007/s11664-017-5547-0.
[122] M.A. Rahman, Design and simulation of a high-performance cd-free Cu2SnSe3 solar cells with SnS electron-blocking hole transport layer and TiO2 electron transport layer by SCAPS-1D, SN Appl. Sci. 3 (2021) 253, https://doi.org/10.1007/s42452-021-04267-3.
[123] K. Nisika, K. Kaur, A.H. Arora, B. Chowdhury, Q. Bahrami, M. Qiao, Energy level alignment and nanoscale investigation of a-TiO2/cu-Zn-Sn-S interface for alternative electron transport layer in earth abundant cu-Zn-Sn-S solar cells, J. Appl. Phys. 126 (2019) 193104, https://doi.org/10.1063/1.5121874.
[124] A. Nisika, K. Ghosh, R.S. Kaur, Q. Bobba, M. Qiao, Engineering Cu2ZnSnS4 grain boundaries for enhanced photovoltage generation at the Cu2ZnSnS4/TiO2 heterojunction: a nanoscale investigation using kelvin probe force microscopy, J. Appl. Phys. 130 (2021) 195301, https://doi.org/10.1063/5.0056161.
[125] R. Yan, L. Kang, Y. Sun, J. Zhang, Solution-processed Cu2ZnSnS4 thin film with mixed solvent and its application in superstrate structure solar cells, RSC Adv. 8 (2018) 11469–11477, https://doi.org/10.1039/C8RA01095A.
[126] S.K. Dwivedi, S.K. Tripathi, D.C. Tiwari, A.S. Chauhan, P.K. Dwivedi, N. Eswara Prasad, Low cost copper zinc tin sulphide (CZTS) solar cells fabricated by sulphurizing sol-gel deposited precursor using 1,2-ethanedithiol (EDT), Sol. Energy 224 (2021) 210–217, https://doi.org/10.1016/j.solener.2021.04.046.